JOURNAL OF THE AMERICAN STATISTICAL ASSOCIATION
2018, VOL. 113, NO. 524, 1565–1582, Theory and Methods
https://doi.org/10.1080/01621459.2017.1356318

Probabilities of Concurrent Extremes

Clément Dombry[a], Mathieu Ribatet [b], and Stilian Stoev[c]

[a]Laboratoire de Mathmatiques de Besanon, Univ. Bourgogne Franche-Comté, UMR CNRS, Besanon, France; [b]Institut Montpelliérain Alexander Grothendieck, University of Montpellier, Montpellier, France; [c]Department of Statistics, University of Michigan, Ann Arbor, MI

ABSTRACT
The statistical modeling of spatial extremes has been an active area of recent research with a growing domain of applications. Much of the existing methodology, however, focuses on the magnitudes of extreme events rather than on their timing. To address this gap, this article investigates the notion of *extremal concurrence*. Suppose that daily temperatures are measured at several synoptic stations. We say that extremes are concurrent if record maximum temperatures occur simultaneously, that is, on the same day for all stations. It is important to be able to understand, quantify, and model extremal concurrence. Under general conditions, we show that the finite sample concurrence probability converges to an asymptotic quantity, deemed *extremal concurrence probability*. Using Palm calculus, we establish general expressions for the extremal concurrence probability through the max-stable process emerging in the limit of the component-wise maxima of the sample. Explicit forms of the extremal concurrence probabilities are obtained for various max-stable models and several estimators are introduced. In particular, we prove that the pairwise extremal concurrence probability for max-stable vectors is precisely equal to the Kendall's τ. The estimators are evaluated from simulations and applied to study temperature extremes in the United States. Results demonstrate that concurrence probability can be used to study, for example, the effect of global climate phenomena such as the El Niño Southern Oscillation (ENSO) or global warming on the spatial structure and areal impact of extremes.

ARTICLE HISTORY
Received March 2016
Revised July 2017

KEYWORDS
Kendall's τ; Max-stable process; Poisson point process; Slyvniak formula; Temperature extremes

1. Introduction

The theory of multivariate and spatial extremes is a rapidly developing area motivated by environmental, climate, or even financial applications, see, for example, the monograph (Finkenstädt and Rootzén 2004) and some recent studies (Cooley, Nychka, and Naveau 2007; Reich and Shaby 2012; Wadsworth and Tawn 2014; Asadi, Davison, and Engelke 2015), to name a few. So far, however, in many applications the prevailing methodology focuses on modeling the magnitudes of the extremes rather than their timing. This can hinder the understanding of the underlying mechanisms giving rise to large values. For example, a popular approach is as follows. Let $X_t(s)$, $t = 1, \dots, n$ be a space-time random field modeling the maximum temperature on day t at site s. In practice, measurements are available at a set of stations $\{s_1, \dots, s_k\} \subset \mathbb{R}^2$. At each location s, define the temporal maxima

$$M_n(s) = \max_{t=1,\dots,n} X_t(s).$$

Assuming weak dependence over time, asymptotic theory (Leadbetter, Lindgren, and Rootzén 1983; Resnick 1987; de Haan and Ferreira 2006) implies that, with suitable location and scale functions $b_n(s)$ and $a_n(s) > 0$,

$$\left\{ \frac{M_n(s) - b_n(s)}{a_n(s)} \right\}_{s\in\mathbb{R}^2} \longrightarrow \{\eta(s)\}_{s\in\mathbb{R}^2}, \quad n \to \infty, \qquad (1)$$

where the limit $\eta = \{\eta(s)\}$ is a max-stable random field, and the convergence is understood in the sense of finite-dimensional distributions. The one-dimensional marginal distributions of η necessarily belong to the generalized extreme value (GEV) family:

$$\mathbb{P}\{\eta(s) \le x\} = \exp\left[-\left\{ 1 + \xi(s) \frac{x - \mu(s)}{\sigma(s)} \right\}_+^{-1/\xi(s)} \right],$$
$$\{\mu(s), \sigma(s), \xi(s)\} \in \mathbb{R} \times (0, \infty) \times \mathbb{R}.$$

From a statistical standpoint, two strategies are possible. A two-step procedure can be used to first estimate the marginal parameters and then, based on these estimates and using the probability integral transform or the empirical distribution, fit a unit Fréchet max-stable process (Davison and Gholamrezaee 2011; Ribatet 2013). A second strategy consists in fitting both the marginal parameter and the spatial dependence structure simultaneously (Padoan, Ribatet, and Sisson 2010; Davison, Padoan, and Ribatet 2012). Either way, the spatial dependence structure is assumed to be one of the available max-stable models, for example, Schlather (Schlather 2002), Extremal-t (Opitz 2013), Brown-Resnick (Kabluchko, Schlather, and de Haan 2009). The fitted max-stable model can then be used to quantify various probabilities of spatial extremes (Davison, Padoan, and Ribatet 2012; Ribatet 2013), do prediction and conditional simulations (Wang and Stoev 2011a; Dombry, Éyi-Minko, and Ribatet 2013; Oesting and Schlather 2013) or downscaling (Oesting, Bel, and Lantuéjoul 2018). Recently Asadi, Davison, and Engelke (2015) extended the methodology to the modeling of river extremes,

CONTACT Mathieu Ribatet mathieu.ribatet@umontpellier.fr Institut Montpelliérain Alexander Grothendieck, University of Montpellier, Montpellier, France.
Color versions of one or more of the figures in the article can be found online at www.tandfonline.com/r/JASA.

where the notion of spatial dependence is expressed in terms of hydrological distance.

The general approach outlined above focuses on the magnitude of extremes. When considering multivariate or spatial extremes over a long period, the occurrence times of extremes at different components or regions become important as well. Indeed practitioners may wonder whether or not the maxima $M_n(s_1)$ and $M_n(s_2)$ at two different sites are achieved *at the same time*. The recent approaches of Wadsworth and Tawn (2014); Engelke et al. (2015) and also the seminal work of Stephenson and Tawn (2005) incorporate more information than the point-wise maximum $\{M_n(s)\}$ field and can help address this issue. In these works, the timing and simultaneous occurrence of extremes arise naturally as ingredients in certain calculations of Poisson process likelihoods (Stephenson and Tawn 2005; Wadsworth and Tawn 2014). So far, however, to the best of our knowledge, the timing or simultaneous occurrence of extremes has received little attention with the notable exception of Ledford and Tawn (1998); Hashorva and Hüsler (2005); Stephenson and Tawn (2005); Wadsworth and Tawn (2014); and Wadsworth (2015).

In this article, we focus on the notion *concurrence of extremes*. Given a sequence $X_1, \ldots, X_n$ of independent copies of a stochastic process $X = \{X(s)\}_{s\in\mathcal{X}}$ defined on a region $\mathcal{X} \subset \mathbb{R}^d$, $d \geq 1$, we say that extremes are *sample concurrent* at locations $s_1, \ldots, s_k \in \mathcal{X}$, $k \geq 2$, if

$$M_n(s_j) = \max_{t=1,\ldots,n} X_t(s_j) = X_{t_0}(s_j), \qquad j = 1, \ldots, k, \qquad (2)$$

for some fixed $t_0 \in \{1, \ldots, n\}$, independent of j. Thus, only one observation $X_{t_0} = \{X_{t_0}(s)\}_{s\in\mathcal{X}}$ is responsible for generating the point-wise maxima at locations $s_1, \ldots, s_k$. The left panel of Figure 1 illustrates the notion of concurrence by showing that extremes are sample concurrent at (s_2, s_3) but not at (s_1, s_2, s_3).

The probability of the sample concurrence event, denoted

$$p_n(s_1, \ldots, s_k) = \mathbb{P}[\text{for some } t_0 \in \{1, \ldots, n\} : M_n(s_j) = X_{t_0}(s_j), \text{for all } j = 1, \ldots, k], \qquad (3)$$

is henceforth referred to as *sample concurrence probability*. Provided that X has continuous margins, it is not difficult to see that

$$p_n(s_1, \ldots, s_k) = n\mathbb{E}\left[F\{X(s_1), \ldots, X(s_k)\}^{n-1}\right],$$

where F is the multivariate cumulative distribution of $\{X(s_1), \ldots, X(s_k)\}$. Interestingly, the concurrence of extremes event is invariant under increasing transformations of the marginals, so $p_n(s_1, \ldots, s_k)$ does not depend on the marginal distributions of X but only on its dependence structure, that is, the copula C associated with F.

One drawback of $p_n(s_1, \ldots, s_k)$ is that it depends on the sample size n, but we will show later in Theorem 1, that, under mild regularity conditions, this quantity stabilizes to a universal large sample limit

$$p_n(s_1, \ldots, s_k) \longrightarrow p(s_1, \ldots, s_k), \qquad n \to \infty. \qquad (4)$$

Throughout this article, we will call the above limiting probability $p(s_1, \ldots, s_k)$ the *extremal concurrence probability*. Note that this result was first established using a different approach by Hashorva and Hüsler (2005, Theorem 2.1, eq. (5))—but see also Gnedin (1993, 1994, 1998). Our approach differentiates from these previous works as it is based on the spectral characterization of max-stable processes. This new approach appears to be an important new insight showing that, for large n, the sample concurrence probability $p_n(s_1, \ldots, s_k)$ can be interpreted as the chance that a single heatwave event affecting all the sites $\{s_1, \ldots, s_k\}$ is responsible for the record maxima. Consequently concurrence probabilities can help understanding and quantifying the areal extent of extreme event.

In Section 2, we make connections between the sample and extremal concurrence probabilities and establish general properties and formula. Section 3 gives closed forms for various parametric max-stable models, and Section 4 introduces various estimators for the sample/extremal concurrence probabilities. The proposed estimators are then analyzed in a simulation study (Section 5) and applied to US continental temperature extremes in Section 6.

2. Concurrence of Extremes

In this section, we show that sample concurrence probabilities converge to extremal concurrence ones under rather mild domain of attraction conditions. We then provide formulas for

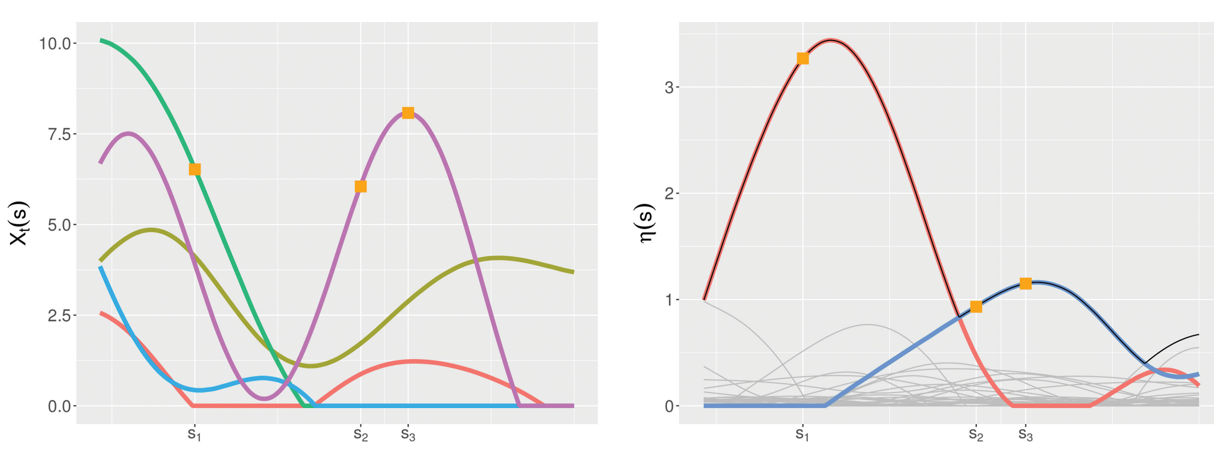

Figure 1. Illustration of the notion of sample (left) and extremal (right) concurrence. In both situations, extremes are concurrent at (s_2, s_3) but not at (s_1, s_2, s_3).

the extremal concurrence probability based on the spectral representation of the associated max-stable process and establish their basic properties.

2.1. Max-Stable Processes and the Definition of Extremal Concurrence

As discussed in the introduction, the sample concurrence probability converges to an asymptotic extremal concurrence probability $p(s_1, \ldots, s_k)$, suggesting that one single (random) function contributes to η at locations $s_1, \ldots, s_k$.

It is well known that every continuous in probability max-stable process η standardized to have unit Fréchet margins has a spectral representation (de Haan 1984; Penrose 1992; Schlather 2002)

$$\eta(s) = \max_{i\geq 1} \zeta_i Y_i(s) \quad s \in \mathcal{X}, \tag{5}$$

where $\{\zeta_i : i \geq 1\}$ are the points of a Poisson process on $(0, \infty)$ with intensity measure $\zeta^{-2}d\zeta$, and Y_i are independent copies of a nonnegative stochastic process such that $\mathbb{E}\{Y(s)\} = 1$ for all $s \in \mathcal{X}$. Standard computations shows that the finite-dimensional distributions of η are

$$\mathbb{P}\{\eta(s_j) \leq z_j,\ j = 1, \ldots, k\} = \exp\left[-\mathbb{E}\left\{\max_{j=1,\ldots,k} \frac{Y(s_j)}{z_j}\right\}\right], \tag{6}$$

where $z_j > 0$, $j = 1, \ldots, k$ (see also Proposition 5.11 in Resnick 1987).

It is often more convenient to rewrite (5) as

$$\eta(s) = \max_{\varphi\in\Phi} \varphi(s), \qquad s \in \mathcal{X}, \tag{7}$$

where $\Phi = \{\varphi_i : i \geq 1\}$ with $\varphi_i = \zeta_i Y_i$ is a Poisson point process on a space of nonnegative functions on $\mathcal{X}$. Following the terminology of Smith (1990), the functions $\varphi \in \Phi$ may be viewed as random "storms," whose component-wise maximum yields the max-stable process η. They may be continuous or discontinuous, depending on the model (see, e.g., Resnick and Roy 1991).

We say that *extremes are concurrent* at $s_1, \ldots, s_k \in \mathcal{X}$ if

$$\eta(s_j) = \varphi_\ell(s_j), \quad j = 1, \ldots, k, \tag{8}$$

for some $\ell \geq 1$. That is, a single spectral function (storm) is responsible for the maximum at all k sites. Similarly to the definition of the sample concurrence probability (3), the extremal concurrence probability is defined by

$$p(s_1, \ldots, s_k) = \mathbb{P}\left\{\text{for some } \ell \geq 1 : \eta(s_j) = \varphi_\ell(s_j),\ j = 1, \ldots, k\right\}. \tag{9}$$

We will show in the next section that the extremal concurrence probability does not depend on the choice of the spectral representation and is well-defined. It turns out that when $k = 2$ the extremal concurrence probability $p(s_1, s_2)$ is precisely the Kendall's τ measure of dependence for the max-stable vector $\{\eta(s_1), \eta(s_2)\}$ (see Theorem 3). In this case, $p(s_1, s_2)$ also coincides with the dependence measure considered in Weintraub (1991) to study mixing properties of max-stable processes.

Interestingly, the extremal concurrence probability shares connections with a widely used dependence measure for extremes known as the bivariate extremal coefficient (Schlather and Tawn 2003; Cooley, Naveau, and Poncet 2006)

$$\theta(s_1, s_2) = -\log \mathbb{P}\{\eta(s_1) \leq 1, \eta(s_2) \leq 1\}, \quad s_1, s_2 \in \mathcal{X}. \tag{10}$$

For instance, Proposition 5.1 in Stoev (2008) implies

$$\frac{1}{2}\{2 - \theta(s_1, s_2)\} \leq p(s_1, s_2) \leq 2\{2 - \theta(s_1, s_2)\}, \tag{11}$$

and we shall see later that the properties of the extremal concurrence probability are similar to that of the extremal coefficient.

2.2. Hitting Scenarios, Sample, and Extremal Concurrence

Concurrence of extremes can be defined through the more general notion of a *hitting scenario* (Wang and Stoev 2011b; Dombry and Éyi-Minko 2013), which reflects precisely how many different events contribute to the componentwise maximum. Let $X_1, \ldots, X_n$ be independent copies of a stochastic process X defined on $\mathcal{X}$ and $s_1, \ldots, s_k \in \mathcal{X}$ be different locations. We suppose that X has continuous marginals to ensure that $\{X_1(s_j), \ldots, X_n(s_j)\}$ has no ties almost surely and that the maximum is uniquely reached. Let $M_n(s) = \max_{i=1,\ldots,n} X_i(s)$ be the componentwise maximum and consider the sets $C_i = \{j : M_n(s_j) = X_i(s_j)\}$, $i = 1, \ldots, n$, that account for the location where the ith component X_i dominates the rest. Some of these sets may be empty, but from the above discussion, with probability one the nonempty ones are disjoint and form a random partition of $\{1, \ldots, k\}$. This partition $\pi_n = \{C_i : C_i \neq \emptyset\}$ will be referred to as the *sample hitting scenario*.

By analogy with extremal concurrence, one can define an *extremal hitting scenario* associated with a max-stable process by using the underlying Poisson point process (Wang and Stoev 2011b; Dombry, Éyi-Minko, and Ribatet 2013; Dombry and Éyi-Minko 2013). More precisely, for η as in (7), the extremal hitting scenario π is defined as the random partition of $\{1, \ldots, k\}$ such that two indices $j_1, j_2 \in \{1, \ldots, k\}$ are in the same component of π if and only if

$$\arg\max_{i\geq 1} \varphi_i(s_{j_1}) = \arg\max_{i\geq 1} \varphi_i(s_{j_2}), \qquad \varphi_i \in \Phi.$$

Whatever type of concurrence is considered, sample concurrence (2) or extremal concurrence (8), extremes are said to be concurrent if and only if $\pi_n = \{1, \ldots, k\}$ or $\pi = \{1, \ldots, k\}$. The next theorem shows the convergence of the sample hitting scenario to the extremal one.

Theorem 1. Assume that $[h_1\{X(s_1)\}, \ldots, h_k\{X(s_k)\}]$ belongs to the maximum domain of attraction of $\{\eta(s_1), \ldots, \eta(s_k)\}$, for some strictly increasing deterministic functions h_i, $i = 1, \ldots, k$. Then, the sample hitting scenario π_n converges in distribution as $n \to \infty$ to the extremal hitting scenario π of the max-stable process η.

The proof is given in the supplementary material.

Corollary 1. If the stochastic process X is in the domain of attraction of some max-stable process η, the sample concurrence probability converges to its extremal counterpart,

$$p_n(s_1,\dots,s_k)=\mathbb{P}[\pi_n=\{1,\dots,k\}]\longrightarrow\mathbb{P}[\pi=\{1,\dots,k\}]=p(s_1,\dots,s_k),\quad n\to\infty,$$

and proves (4).

Remark 1. This result, and in fact, a concrete formula for the concurrence probability was first obtained by Hashorva and Hüsler (2005, Theorem 2.1) with different methods. Our Theorem 1 extends these results to the convergence of hitting scenarios, where our proof involves point process limits and continuous mapping.

2.3. General Formulas for the Extremal Concurrence Probabilities

The following theorem gives an expression for the extremal concurrence probability $p(s_1,\dots,s_k)$.

Theorem 2. We have

$$p(s_1,\dots,s_k)=\mathbb{E}_Y\left(\left[\mathbb{E}_{\tilde Y}\left\{\max_{j=1,\dots,k}\frac{\tilde Y(s_j)}{Y(s_j)}\right\}\right]^{-1}\right),\tag{12}$$

where Y and $\tilde Y$ are independent copies of the stochastic process appearing in (5).

Alternatively, we also have

$$p(s_1,\dots,s_k)=\sum_{r=1}^{k}(-1)^r\sum_{\substack{J\subseteq\{1,\dots,k\}\\|J|=r}}\mathbb{E}_{\tilde\eta}\left[\log\mathbb{P}_\eta\left\{\eta(s_j)\le\tilde\eta(s_j),\ j\in J\right\}\right],\tag{13}$$

where $\tilde\eta$ is an independent copy of η.

Proof. We consider here only the proof of (12). The proof of (13) is given in the supplementary material.

It suffices to restrict the representation (7) to the space $\mathbb{R}_+^k$, corresponding to coordinates $s_1,\dots,s_k$. Let Λ denote the intensity measure of the Poisson point process Φ induced on $\mathbb{R}_+^k$:

$$\Lambda(A)=\int_0^\infty\mathbb{P}\left[\left\{\zeta Y(s_j):j=1,\dots,k\right\}\in A\right]\zeta^{-2}d\zeta,$$

for all Borel sets $A\subset\mathbb{R}_+^k$. We have by the Slyvniak–Mecke formula (see, e.g., Schneider and Weil 2008, p. 68) that

$$\begin{aligned}p(s_1,\dots,s_k)&=\mathbb{P}\{\exists\varphi\in\Phi:\varphi(s_1)=\eta(s_1),\dots,\varphi(s_k)=\eta(s_k)\}\\&=\int_{\mathbb{R}_+^k}\mathbb{P}\left\{\tilde\eta(s_j)<x_j,\ j=1,\dots,k\right\}\Lambda(dx_1,\dots,dx_k),\end{aligned}\tag{14}$$

where $\tilde\eta$ is an independent copy of η. Using the form of the intensity of Φ in the right-hand side of (14), we further obtain

$$\begin{aligned}p(s_1,\dots,s_k)&=\mathbb{E}_Y\left[\int_0^\infty\mathbb{P}\left\{\tilde\eta(s_j)<\zeta Y(s_j),\ j=1,\dots,k\right\}\zeta^{-2}d\zeta\right]\\&=\mathbb{E}_Y\left(\int_0^\infty\exp\left[-\mathbb{E}_{\tilde Y}\left\{\max_{j=1,\dots,k}\frac{\tilde Y(s_j)}{\zeta Y(s_j)}\right\}\right]\zeta^{-2}d\zeta\right)\\&=\mathbb{E}_Y\left(\left[\mathbb{E}_{\tilde Y}\left\{\max_{j=1,\dots,k}\frac{\tilde Y(s_j)}{Y(s_j)}\right\}\right]^{-1}\right).\end{aligned}$$

In the second relation, we used the expression (6) with $\tilde Y$ an independent copy of Y and the last relation follows from the fact that $\int_0^\infty e^{-a/\zeta}\zeta^{-2}d\zeta=a^{-1},\ a>0.$ □

Remark 2. By the seminal article of de Haan (1984) (see also Stoev and Taqqu 2005; Kabluchko 2009), any continuous in probability max-stable process can be represented as

$$\{\eta(s):s\in\mathcal{X}\}\overset{\mathrm{d}}{=}\left\{\max_{i\ge1}\zeta_i f_s(u_i):s\in\mathcal{X}\right\},\tag{15}$$

where $\{f_s:s\in\mathcal{X}\}$ is a collection of nonnegative integrable functions on the space $(U,\mathcal{U},\nu)$. Here $\{(\zeta_i,u_i):i\ge1\}$ is a Poisson point process on $(0,\infty)\times U$ with intensity $\zeta^{-2}d\zeta\,\nu(du)$. The functions $\{f_s:s\in\mathcal{X}\}$ are known as *spectral functions* of η and (15) as de Haan's spectral representation. When ν is a probability measure, one can view $Y(s)=f_s$ as random variables on the probability space $(U,\mathcal{U},\nu)$ and then (15) becomes (5). Conversely, any representation (15) can be cast in the form (5) with a change of variables. Depending on the context one representation may be more convenient than the other. In terms of (15), the concurrence probability formula in (12) becomes

$$p(s_1,\dots,s_k)=\int_U\left[\int_U\left\{\max_{j=1,\dots,k}\frac{f_{s_j}(\tilde u)}{f_{s_j}(u)}\right\}\nu(d\tilde u)\right]^{-1}\nu(du),\tag{16}$$

and the proof is essentially the same.

Remark 3. The notions of sample and extremal concurrence can be naturally extended to infinite sets of sites $K\subset\mathcal{X}$. Barring measurability details, the proof of Theorem 2 remains the same and formula (12) becomes

$$p(K)=\mathbb{E}_Y\left(\left[\mathbb{E}_{\tilde Y}\left\{\sup_{s\in K}\frac{\tilde Y(s)}{Y(s)}\right\}\right]^{-1}\right),\tag{17}$$

provided that the underlying suprema of stochastic processes are well-defined random variables. Here, for simplicity of exposition, we focus on the case of concurrence over finitely many sites, which requires no joint measurability assumptions on $Y(\cdot)$ and is sufficient for most practical applications. For further theoretical treatment of concurrence over regions, see Dombry, Falk, and Zott (2015).

In the bivariate case $k=2$, Equation (13) reads

$$p(s_1,s_2)=2+\mathbb{E}_{\tilde\eta}\left[\log\mathbb{P}_\eta\left\{\eta(s_j)\le\tilde\eta(s_j),\ j=1,2\right\}\right].\tag{18}$$

This entails the very unexpected result that the bivariate extremal concurrence probability equals the well-known Kendall's τ.

Theorem 3. For any max-stable process η, we have

$$\begin{aligned}p(s_1,s_2)&=\tau_{\{\eta(s_1),\eta(s_2)\}}\\&\equiv\mathbb{E}\left[\mathrm{sign}\{\eta(s_1)-\eta_\star(s_1)\}\mathrm{sign}\{\eta(s_2)-\eta_\star(s_2)\}\right]\end{aligned}$$

is the Kendall's τ of $\{\eta(s_1), \eta(s_2)\}$ and $\eta_\star$ is an independent copy of η.

Proof. Let $W = F\{\eta(s_1), \eta(s_2)\}$ where F is the bivariate cumulative distribution function of $\{\eta(s_1), \eta(s_2)\}$. From (18) we have $p(s_1, s_2) = 2 + \mathbb{E}(\log W)$. But since $\{\eta(s_1), \eta(s_2)\}$ is a bivariate max-stable random vector, we know that $\mathbb{P}(W \leq w) = w - (1-\tau)w \log w$, $0 \leq w \leq 1$ (Ghoudi, Khoudraji, and Rivest 1998) and hence, after some simple calculations, $p(s_1, s_2) = \tau$. □

2.4. Properties of Extremal Concurrence Probabilities

In the remaining part of this section, we investigate some properties of the extremal concurrence probabilities. Surprisingly, although the two notions are different, we encounter strong connections with the extremal coefficient (10). We recall that the extremal coefficient $\theta(s_1, s_2)$ takes values in $[1, 2]$, the lower and upper bounds correspond to perfect dependence and independence, respectively. The next proposition states a similar result for the extremal concurrence probability.

Proposition 1. For all $s_1, s_2 \in \mathcal{X}$, we have
(i) $p(s_1, s_2) = 0$ if and only if $\eta(s_1)$ and $\eta(s_2)$ are independent;
(ii) $p(s_1, s_2) = 1$ if and only if $\eta(s_1)$ and $\eta(s_2)$ are almost surely equal.

The proof uses the following generalization and improvement of the upper bound in (11).

Lemma 1. For all $s_1, \dots, s_k \in \mathcal{X}, k \geq 2$, we have $p(s_1, \dots, s_k) \leq \mathbb{E}\{\min_{j=1,\dots,k} Y(s_j)\}$.

Proof. In the context of Theorem 2, we have (by conditioning on Y)

$$\mathbb{E}_{\tilde{Y}}\left\{\max_{j=1,\dots,k} \frac{\tilde{Y}(s_j)}{Y(s_j)}\right\} \geq \max_{j=1,\dots,k} Y(s_j)^{-1}\mathbb{E}_{\tilde{Y}}\{\tilde{Y}(s_j)\} = \left\{\min_{j=1,\dots,k} Y(s_i)\right\}^{-1},$$

since $\mathbb{E}_{\tilde{Y}}\{\tilde{Y}(s_j)\} = 1$. This, in view of (12) implies the desired result. □

Proof of Proposition 1. Equation (11) implies that $p(s_1, s_2) = 0$ if and only if $\theta(s_1, s_2) = 2$ which is equivalent to the independence of $\eta(s_1)$ and $\eta(s_2)$. When $p(s_1, s_2) = 1$, Lemma 1 entails $Y(s_1) = Y(s_2)$ almost surely so that $\eta(s_1) = \eta(s_2)$ almost surely, because $Y(s_i) \geq 0$, $i = 1, 2$ and $\mathbb{E}\{Y(s_1)\} = \mathbb{E}\{Y(s_2)\} = 1$. It is easy to prove the converse implication: if $\eta(s_1)$ and $\eta(s_2)$ are almost surely equal, the same holds for $Y(s_1)$ and $Y(s_2)$ so that $p(s_1, s_2) = 1$. □

Interestingly $p(s_1, \dots, s_k)$ can be expressed via the extremal coefficients of another max-stable process.

Proposition 2. Let $\tilde{\eta}, \tilde{\eta}_1, \tilde{\eta}_2, \dots$ be independent copies of the max-stable process η defined in (5) and consider the simple max-stable process

$$\xi(s) = \max_{i \geq 1} \zeta_i \frac{Y_i(s)}{\tilde{\eta}_i(s)}, \qquad s \in \mathcal{X}.$$

We have

$$p(s_1, \dots, s_k) = \sum_{r=1}^{k} (-1)^{r+1} \sum_{\substack{J \subseteq \{1,\dots,k\} \\ |J| = r}} \theta_\xi(s_j, j \in J), \qquad (19)$$

where $\theta_\xi(s_j, j \in J) = -\log \mathbb{P}\{\xi(s_j) \leq 1, j \in J\}$ and in particular,

$$p(s_1, s_2) = 2 - \theta_\xi(s_1, s_2).$$

Proof. Clearly ξ is a simple max-stable process since both Y and $\tilde{\eta}$ are nonnegative and $\mathbb{E}\{Y(s)/\tilde{\eta}(s)\} = 1$ for all $s \in \mathcal{X}$. We have

$$\begin{aligned}
&\mathbb{E}_{\tilde{\eta}}\left[\log \mathbb{P}_\eta\left\{\eta(s_j) \leq \tilde{\eta}(s_j), j \in J\right\}\right] \\
&= -\mathbb{E}_{\tilde{\eta}}\left[\mathbb{E}_Y\left\{\max_{j \in J} \frac{Y(s_j)}{\tilde{\eta}(s_j)}\right\}\right] \\
&= \log \mathbb{P}_\xi\left\{\xi(s_j) \leq 1, j \in J\right\} = -\theta_\xi(s_j, j \in J),
\end{aligned}$$

and (19) follows from (13). □

The next corollary lists some properties of the extremal concurrence probability function that closely parallel those of the extremal coefficient function. In view of Proposition 2, the proof follows from Schlather and Tawn (2003) or Cooley, Naveau, and Poncet (2006).

Corollary 2. Let $p : h \mapsto p(o, h)$ be an extremal concurrence probability function associated with a stationary max-stable process in $\mathcal{X}$ for some arbitrary origin $o \in \mathcal{X}$ and $h \in \mathcal{X}$. Then the following assertions hold.
(i) The function $h \mapsto p(h)$ is positive semidefinite;
(ii) The function $h \mapsto p(h)$ is not differentiable at the origin unless $p(h) = 1$ for all $h \in \mathcal{X}$;
(iii) If $d \geq 1$ and if η is isotropic, then $h \mapsto p(h)$ has at most a jump at the origin and is continuous elsewhere;
(iv) $\{2 - p(h_1 + h_2)\} \leq \{2 - p(h_1)\}\{2 - p(h_2)\}$ for all $h_1, h_2 \in \mathcal{X}$;
(v) $\{2 - p(h_1 + h_2)\}^\alpha \leq \{2 - p(h_1)\}^\alpha + \{2 - p(h_2)\}^\alpha - 1$ for all $h_1, h_2 \in \mathcal{X}$ and $0 \leq \alpha \leq 1$;
(vi) $\{2 - p(h_1 + h_2)\}^\alpha \geq \{2 - p(h_1)\}^\alpha + \{2 - p(h_2)\}^\alpha - 1$ for all $h_1, h_2 \in \mathcal{X}$ and $\alpha < 0$.

2.5. Integrated Concurrence Probabilities and Area of Concurrence Cell

As we will see in Sections 4 and 6, one can provide simple estimators of the bivariate concurrence probabilities and establish bivariate concurrence probability maps $s \mapsto p(s_0, s)$ centered at a given location s_0. Such maps show how fast the dependence in extremes decreases when moving away from s_0. A drawback of this approach is that one may produce one such map for every choice of an origin s_0 and the choice of an origin is hence quite arbitrary. To bypass this issue, we propose to consider the integrated concurrence probability

$$I(s_0) = \int_{s \in \mathcal{X}} p(s_0, s) ds, \qquad s_0 \in \mathcal{X}.$$

Intuitively, this quantity measures how fast the dependence in extremes decreases when moving away from s_0. Interestingly, it can be related to the notion of *concurrence cell*. Consider the spectral representation (7) and recall that we have a concurrence of extremes at sites s_0 and s if $\eta(s_0) = \varphi(s_0)$ and $\eta(s) = \varphi(s)$, for the same $\varphi \in \Phi$. Let $C(s_0)$ denotes the *random* set of all sites s that are in a concurrence relation with s_0. This set will be referred to as the *concurrence cell* containing the site s_0.

Proposition 3. For any site $s_0 \in \mathcal{X}$, let $|C(s_0)|$ be the d-dimensional volume of $C(s_0)$. We have

$$\mathbb{E}\{|C(s_0)|\} = I(s_0) \quad \text{and}$$
$$\text{var}\{|C(s_0)|\} = \int_{\mathcal{X}^2} \{p(s_0, s_1, s_2) - p(s_0, s_1)p(s_0, s_2)\} ds_1 ds_2.$$

Proof. Observe that the concurrence probability satisfies $p(s_0, s) = \mathbb{E}\{1_{C(s_0)}(s)\}$ and that the volume of the concurrence cell is given by $|C(s_0)| = \int_{\mathcal{X}} 1_{C(s_0)}(s)ds$. The formula $\mathbb{E}\{|C(s_0)|\} = I(s_0)$ follows by applying the Tonelli–Fubini's theorem. Similarly for the variance, we have

$$\begin{aligned}
&\text{var}\{|C(s_0)|\} \\
&= \mathbb{E}\{|C(s_0)|^2\} - [\mathbb{E}\{|C(s_0)|\}]^2 \\
&= \mathbb{E}\left\{\int_{\mathcal{X}^2} 1_{C(s_0)}(s_1) 1_{C(s_0)}(s_2) ds_1 ds_2\right\} - I(s_0)^2 \\
&= \int_{\mathcal{X}^2} p(s_0, s_1, s_2) ds_1 ds_2 - \int_{\mathcal{X}^2} p(s_0, s_1)p(s_0, s_2) ds_1 ds_2.
\end{aligned}$$
□

We will provide and discuss in Section 6 some maps of the integrated concurrence probability $s_0 \mapsto I(s_0)$ that allow to evaluate at each location s_0 the dependence in extremes around s_0. For a detailed study of the properties of the concurrence cells associated with a max-stable random field and of the tessellation of the entire domain generated by the concurrence cells, please refer to the recent work of Dombry and Kabluchko (2017).

3. Extremal Concurrence Probabilities for Specific Models

In this section, we gather formulas for the extremal concurrence probabilities for some popular models of max-stable random vectors and processes. As we will see, it is not always possible to get explicit formulas, and in such situations, we propose to use Monte Carlo approximation methods. Proofs related to this section are given in the supplementary material and mainly rely on Theorem 2.

3.1. Closed-Form Expressions

Example 1 (Logistic model). Consider the k-variate logistic model, that is, with cumulative distribution

$$F(z_1, \ldots, z_k) = \exp\left\{-\left(\sum_{j=1}^{k} z_j^{-1/\alpha}\right)^{\alpha}\right\}, \quad 0 < \alpha \leq 1, \quad z_1, \ldots, z_k > 0.$$

Its concurrence probability is given by

$$p(s_1, \ldots, s_k) = \prod_{j=1}^{k-1}(1 - \alpha/j).$$

Recall that independence is reached when $\alpha = 1$ while perfect dependence occurs as $\alpha \downarrow 0$ and, as expected, for such situations we have $p(s_1, \ldots, s_k) = 0$ and $p(s_1, \ldots, s_k) = 1$, respectively.

Example 2 (Max-linear model). Consider the max-linear model $\eta(s) = \max_{m=1,\ldots,n} \varphi_m(s) Z_m$, where $Z_1, \ldots, Z_n$ are independent standard unit Fréchet random variables and some nonnegative functions $\varphi_m(s)$, $m = 1, \ldots, n$, such that $\sum_{m=1}^{n} \varphi_m(s) = 1$ for all $s \in \mathcal{X}$. We have

(i) The concurrence probability equals

$$p(s_1, \ldots, s_k) = \sum_{\ell=1}^{n} p_\ell(s_1, \ldots, s_k),$$
$$p_\ell(s_1, \ldots, s_k) = \left\{\sum_{m=1}^{n} \max_{j=1,\ldots,k} \frac{\varphi_m(s_j)}{\varphi_\ell(s_j)}\right\}^{-1}, \quad (20)$$

with the convention that $0/0 = 0$, $a/0 = \infty$ if $a > 0$.

(ii) The probability that component ℓ dominates at sites $s_1, \ldots, s_k$ is given by the term p_ℓ in (20), that is,

$$p_\ell(s_1, \ldots, s_k) = \mathbb{P}\left\{\eta(s_j) = \varphi_\ell(s_j) Z_\ell, \ j = 1, \ldots, k\right\}. \quad (21)$$

Example 3 (Chentsov random fields). Suppose that the process $Y(s) = 1_A(s)$, where $A \subset \mathbb{R}^d$ is a random set. Then, by analogy with the theory of symmetric α-stable process (Samorodnitsky and Taqqu 1994, chap. 8), we introduce the max-stable process

$$\eta(s) = \max_{i \geq 1} \zeta_i 1_{A_i}(s), \qquad s \in \mathcal{X},$$

where $Y_i \equiv 1_{A_i}$ are independent copies of $Y \equiv 1_A$. The process η will be referred to as a *Chentsov-type max-stable random field* on $\mathcal{X}$.

For a Chentsov-type max-stable process, we have

$$p(s_1, \ldots, s_k) = \mathbb{P}\left(\{s_1, \ldots, s_k\} \subset A \mid \{s_1, \ldots, s_k\} \cap A \neq \emptyset\right), \quad (22)$$

or less formally, the extremal concurrence probability is the conditional probability that all the sites $s_1, \ldots, s_k$ are covered by the random set A given that at least one of the sites is covered.

Example 4 (Extremal processes). Recall that the max-stable process $\{\eta(s) : s \in [0, 1]\}$ is an extremal process if it has stationary and independent max-increments, that is,

$$\{\eta(s_1), \ldots, \eta(s_k)\} \stackrel{\text{d}}{=} [s_1 Z_1, \max\{s_1 Z_1, (s_2 - s_1) Z_2\}, \ldots, \max\{s_1 Z_1, \ldots, (s_k - s_{k-1}) Z_k\}],$$

where $0 < s_1 < \cdots < s_k$ and $Z_1, \ldots, Z_k$ are independent unit Fréchet random variables (see, e.g., chap. 4.3 in Resnick 1987). It can be shown that

$$\{\eta(s), \ s \in [0, 1]\} \stackrel{\text{d}}{=} \left\{\max_{i \geq 1} \zeta_i 1_{[U_i, 1]}(s), \ s \in [0, 1]\right\},$$

where U_i's are independent $U(0, 1)$ random variables. Using our previous result on Chentsov-type random fields, with $A := [U, 1]$ where $U \sim U(0, 1)$, we have for all $0 < s_1 < \cdots < s_k \leq 1$

$$p(s_1, \ldots, s_k) = \frac{\mathbb{P}\left(\{s_1, \ldots, s_k\} \subset [U, 1]\right)}{\mathbb{P}\left(\{s_1, \ldots, s_k\} \cap [U, 1] \neq \emptyset\right)} = \frac{\mathbb{P}(U \leq s_1)}{\mathbb{P}(U \leq s_k)} = \frac{s_1}{s_k}.$$

This result is not surprising since for this simple case, extremes are concurrent at locations $0 < s_1 < \cdots < s_k < 1$ if $\eta(s)$ has no jumps in the interval $[s_1, s_k]$. Hence using the independence and stationarity of the max-increments, the probability of the latter event is $\mathbb{P}\{s_1 Z_1 \geq (s_k - s_1)Z_2\} = s_1/s_k$, where Z_1 and Z_2 are two independent standard unit Fréchet variables.

Example 5 (Indicator moving maxima). In the context of (15), if $f_s(u) = 1_{A_s}(u)$, for some sequence of measurable *deterministic sets* A_s, by using (16), we obtain as in (1) that

$$p(s_1, \dots, s_k) = \frac{\nu(\cap_{j=1,\dots,k} A_{s_j})}{\nu(\cup_{j=1,\dots,k} A_{s_j})}. \tag{23}$$

In the simple case $f_s(u) = 1_A(u - s)$, that is, $A_s = s + A$ with some deterministic set A, where ν is the Lebesgue measure on $\mathbb{R}^d$, relation (23) implies

$$p(s, s+h) = p(h) = \frac{|A \cap (h + A)|}{|A \cup (h + A)|} = \frac{c_A(h)}{2|A| - c_A(h)},$$

where $|A|$ denotes the d-dimensional volume of A and $c_A(h) = |A \cap (h + A)|$. The latter function and hence the extremal concurrence probability function $p(h)$ can then be obtained in closed form for many different sets. For example, in the case η is isotropic, that is, $A = \{s \in \mathbb{R}^d : \|x\| \leq r\}$ is the centered ball of radius $r > 0$ in Euclidean space, using the formula for the volume of the cap, we obtain

$$c_A(\|h\|) = C_d r^d B_{(d+1)/2, 1/2}\left\{\frac{\|h\|(2r - \|h\|)}{2r^2}\right\},$$
$$C_d = \frac{\pi^{d/2}}{\Gamma(1 + d/2)},$$

where $B_{a,b}(x) = B(a, b)^{-1} \int_0^x u^{a-1}(1-u)^{b-1} du$ is the cumulative distribution function of a Beta(a, b) random variable.

3.2. Numerical Approximations

It may happen that for some parametric max-stable models, explicit forms for extremal concurrence probabilities are not available but hopefully it is often possible to use Monte Carlo methods to approximate the theoretical extremal concurrence probabilities with arbitrary precision. A naive strategy would consist in using (12) to devise a Monte Carlo estimator, but it is wiser to take advantage of the closed forms of max-stable processes cumulative distributions, that is,

$$\mathbb{P}\left\{\eta(s_j) \leq z_j, j = 1, \dots, k\right\} = \exp\{-V_{s_1,\dots,s_k}(z_1, \dots, z_k)\},$$
$$z_1, \dots, z_k > 0,$$

where $V_{s_1,\dots,s_k}$ is an homogenous function of order -1. Rewriting (12), we found

$$\begin{aligned} &p(s_1, \dots, s_k) \\ &= \mathbb{E}_Y\left(\left[-\log \mathbb{P}_{\tilde{\eta}}\left\{\tilde{\eta}(s_j) \leq Y(s_j), j = 1, \dots, k\right\}\right]^{-1}\right) \\ &= \mathbb{E}_Y\left(\left[V_{s_1,\dots,s_k}\{Y(s_1), \dots, Y(s_k)\}\right]^{-1}\right) \end{aligned} \tag{24}$$

which can easily be estimated by sampling independent copies of Y and computing the sample mean. We can often make use of antithetic variables to get more precise estimates. Note that specific choice of the spectral process Y can lead to better strategies as we will illustrate in the following examples.

Example 6 (Brown–Resnick model). Let η be a Brown–Resnick stationary random field on $\mathcal{X}$ driven by a Gaussian process (Kabluchko, Schlather, and de Haan 2009). That is, the processes Y_i in (5) are equal in distribution to

$$Y(s) = \exp\{W(s) - \gamma(s)\}, \qquad s \in \mathcal{X}, \tag{25}$$

where W is a zero mean Gaussian random field with stationary increments and semivariogram γ, that is, $2\gamma(h) = \mathbb{E}\{W(h)^2\} = \mathbb{E}[\{W(s+h) - W(s)\}^2]$, $s, h \in \mathcal{X}$.

For this model, the bivariate extremal concurrence probability function is given by

$$p(o, h) = \mathbb{E}([\Phi(Z) + \exp\{\gamma(h) - \sqrt{2\gamma(h)}Z\}\Phi\{\sqrt{2\gamma(h)} - Z\}]^{-1}), \tag{26}$$

where $Z \sim N(0, 1)$ has the standard normal distribution with cumulative distribution function Φ. As expected $p(o) = 1$ and $p(h) \to 0$ as $\|h\| \to \infty$ provided that the semivariogram is unbounded, that is, $\gamma(h) \to \infty$ as $\|h\| \to \infty$.

Example 7 (Schlather and extremal-t processes). Let η be an extremal-t process on $\mathcal{X}$, that is, the processes Y_i in (5) are equal in distribution to

$$Y(x) = c_\nu \max\{0, W(s)\}^\nu,$$
$$c_\nu = \sqrt{\pi} 2^{-(\nu-2)/2} \Gamma\left(\frac{\nu+1}{2}\right)^{-1} \qquad s \in \mathcal{X},$$

where $\nu \geq 1$ and W is a stationary standard Gaussian process with correlation function ρ. The Schlather process is obtained when $\nu = 1$.

The corresponding extremal concurrence probability function $p(o, h)$ equals

$$\begin{aligned} \mathbb{E}\Bigg(\Bigg[&T_{\nu+1}(T) + \{\rho(h) + \sigma(h)T\}^{-\nu} T_{\nu+1} \\ &\times \left\{-\frac{\rho(h)}{\sigma(h)} + \frac{1}{\sigma(h)(\rho(h) + \sigma(h)T)}\right\}\Bigg]^{-1} 1_{\{\rho(h)+\sigma(h)T>0\}}\Bigg), \end{aligned} \tag{27}$$

where $\sigma(h) = \sqrt{\{1 - \rho(h)^2\}/(1 + \nu)}$ and T is a Student random variable with $\nu + 1$ degrees of freedom and cumulative distribution function $T_{\nu+1}$.

Remark 4. The previous two examples provide useful tools for statistical inference. In practice, one can fit a Brown–Rescnick or extremal-t max-stable process model to data by using, for example, the composite likelihood approach of Padoan, Ribatet, and Sisson (2010). Then, the concurrence probability function is readily obtained via Monte Carlo methods from (26) or (27).

4. Statistical Inference and Asymptotic Properties

4.1. Sample Concurrence Probability Estimators

We define a sample concurrence probability estimator by dividing data into blocks and study its basic properties as well as the optimal choice of the block-size.

Let $X_i = \{X_i(s_j) : j = 1, \ldots, k\}$, $i = 1, \ldots, n$, be random vectors in $\mathbb{R}^k$, $k \geq 2$. Partition the data into nonoverlapping blocks of size $m < n$, and define the *sample concurrence probability estimator*

$$\hat{p}_m \equiv \hat{p}_m(X_1, \ldots, X_n) = \frac{1}{[n/m]} \sum_{r=1}^{[n/m]} 1_{\{\text{sample concurrence in block } r\}}, \quad (28)$$

where, as in (2), we have

$$\{\text{sample concurrence in block } r\} = \left\{ \max_{i=1,\ldots,m} X_{i+(r-1)m} = X_{\ell+(r-1)m} \text{ for some } \ell = 1, \ldots, m \right\},$$

that is one vector in the rth block dominates the others.

Assuming that $X_1, \ldots, X_n$ are independent and identically distributed, the above estimator is the sample mean of $[n/m]$ independent Bernoulli(p_m) random variables, where p_m is as in (3) with n replaced by m. Therefore,

$$\mathbb{E}(\hat{p}_m) = p_m, \qquad \text{var}(\hat{p}_m) = \frac{p_m(1-p_m)}{[n/m]},$$

that is, $\hat{p}_m$ is a unbiased estimator for p_m.

As argued in the introduction, a major drawback of the sample concurrence probability p_m is that it depends on the sample size m and it is thus more sensible to focus on the limiting *extremal concurrence probability* $p = p(s_1, \ldots, s_k)$. If X in the max-domain of attraction of some multivariate max-stable distribution, we know from Corollary 1 that $p_m \to p$ as $m \to \infty$. However, the sample concurrence probability estimator $\hat{p}_m$ is biased for p with mean squared error

$$\text{MSE}(\hat{p}_m) = (p_m - p)^2 + \frac{p_m(1-p_m)}{[n/m]}. \quad (29)$$

We encounter here a typical bias-variance trade off: while the bias $p_m - p$ vanishes as $m \to \infty$, the variance grows asymptotically linearly with m with rate $p(1-p)m/n$. The optimal block size m in terms of mean squared error depends strongly of the behavior the bias function $p_m - p$ which in general cannot be evaluated except if we assume a max-domain of attraction condition—see Section 4.2.

Still, assuming a particular rate of decay for the bias, we can study the bias-variance trade off further. Assuming $0 < p < 1$ and $p_m - p \sim cm^{-\delta}$ for some $c, \delta > 0$, we obtain

$$\text{MSE}(\hat{p}_m) = \left(\frac{c}{m^\delta}\right)^2 + \frac{p(1-p)m}{n} + o(m^{-2\delta}) + o(m/n).$$

Taking the derivative with respect to m, we see that the minimal MSE corresponds to the optimal block size

$$m_{\text{opt}} \sim \left\{ \frac{2\delta c^2 n}{p(1-p)} \right\}^{1/(2\delta+1)}, \qquad n \to \infty. \quad (30)$$

The corresponding mean squared error is $\text{MSE}(\hat{p}_{m_{\text{opt}}}) \propto n^{-2\delta/(2\delta+1)}$.

The asymptotic behavior of the estimator $\hat{p}_m$ is given in the following theorem.

Theorem 4. Assume $p_m - p \sim cm^{-\delta}$ for some constants c, $\delta > 0$.

(i) Suppose $0 < p < 1$ and let $m = m(n)$ be such that $n/m(n) \to \infty$ and $m(n)/n^{1/(2\delta+1)} \to \lambda \in (0, \infty]$, as $n \to \infty$. Then, we have

$$\sqrt{n/m}(\hat{p}_m - p) \longrightarrow N\left\{ \frac{c}{\lambda^{\delta+1/2}}, p(1-p) \right\}, \qquad n \to \infty,$$

with $1/\infty$ being interpreted as zero.

(ii) Suppose that $p = 0$ and let $m = m(n)$ be such that $n/m(n) \to \infty$ and $m(n)/n^{1/(\delta+1)} \to \lambda \in (0, \infty]$ as $n \to \infty$. If $\lambda < \infty$, then

$$(n/m)\hat{p}_m \longrightarrow \text{Poisson}(c/\lambda^{\delta+1}), \qquad n \to \infty.$$

Otherwise, if $\lambda = \infty$, then $\mathbb{P}(\hat{p}_m = 0) \to 1$ as $n \to \infty$.

The proof can be found in the supplementary materials.

Remark 5. In part (i) of Theorem 4, the case $\lambda < \infty$ yields the optimal rate of convergence $n^{\delta/(2\delta+1)}$ but a bias term $c\lambda^{-\delta-1/2}$ appears in the limit. On the other hand, the rate sub-optimal choice $\lambda = \infty$ yields unbiased normal limit.

4.2. Behavior Under Max-Stability

In the previous section, we assumed that the bias $p_m - p$ decays as a power function. This can indeed be assumed for max-stable data, as shown in the following proposition.

Proposition 4. Assume that X is max-stable.

(i) The bias $p_m - p$ is nonincreasing in m and satisfies $0 \leq p_m - p \leq (1-p)/m$, $m \geq 1$.
(ii) In the bivariate case $k = 2$, we have $p_m - p = (1-p)/m$, $m \geq 1$.
(iii) If $0 < p < 1$, then $p_m - p \sim cm^{-\delta}$ as $m \to \infty$, for some $\delta \in \{1, \ldots, k-1\}$ and $c \in (0, 1-p]$.

The proof relies on an exact formula for $(p_m - p)$ via the distribution of the extremal hitting scenario and is given in the supplementary material.

Note that in part (iii) of Proposition 4, the case $\delta \geq 2$ corresponds to peculiar dependence structure, the standard case being rather $\delta = 1$, that is, $p_m - p \sim cm^{-1}$ with $0 < c < 1 - p$—see Lemma 1.1 in the supplement. According to (30), the optimal block size is then of order $n^{1/3}$ and the minimum MSE of order $n^{-2/3}$. For the rate optimal block size $m \sim \lambda n^{1/3}$, Theorem 4 part (i) with $\delta = 1$ and $c > 0$ yields

$$n^{1/3}(\hat{p}_m - p) \longrightarrow N\left\{ \frac{c}{\lambda^{3/2}}, p(1-p) \right\}, \qquad n \to \infty.$$

Note that in all cases, the bias $p_m - p$ is dominated by $1/m$ so that the choice of block size $m = n^{1/3}$ is conservative and ensures an MSE of order $n^{-2/3}$.

In the bivariate max-stable case, the bias is exactly $p_m - p = (1-p)/m$ (see part ii) of Proposition 4. This allows us to propose a bias correction and, in fact, to reach the parametric rate of convergence of order $\sqrt{n}$.

Corollary 3. In the bivariate max-stable case, the estimator

$$\tilde{p}_m = \frac{m\hat{p}_m - 1}{m - 1}$$

is unbiased for p. Furthermore, for any fixed $m \geq 2$,

$$\sqrt{n}(\tilde{p}_m - p) \longrightarrow N\left\{0, m(1-p)(p+1/(m-1))\right\}.$$

The proof is similar to that of Theorem 4. A routine calculation yields that in this case the variance-optimal choice of the block size is the largest integer m, such that $m(m-1) < 1/p$, that is, $m_{\text{opt}} \approx 1 + 1/\sqrt{p}$.

4.3. The Permutation Bootstrap

We propose here a methodological improvement of the sample concurrence probability estimator $\hat{p}_m$ based on permutation bootstrap. The idea is to compute the estimator $\hat{p}_m$ for several independent random permutations of the sample $X_1, \dots, X_n$. Then the average of the resulting estimator would have a lower variance and the same mean p_m.

Formally, this procedure is justified by the following simple observation based on the Rao–Blackwell theorem. Consider the *lexicographic* linear order in $\mathbb{R}^k$, denoted $\prec$, and let $X_{(1)} \prec X_{(2)} \prec \cdots \prec X_{(n)}$ be the sorted sample obtained from $X_1, \dots, X_n$. The independence of the X_i's and the continuity of their marginals entails that the above ordering is strict with probability one. Let $T\{X_1, \dots, X_n\} = (X_{(1)}, \dots, X_{(n)})$. It can be shown that T is a *sufficient statistic* for the parameter $p_m = p_m(s_1, \dots, s_k)$ and the Rao–Blackwell theorem implies the following proposition. Its proof can be found in the supplementary material.

Proposition 5. For $\hat{p}^\star_m = \mathbb{E}(\hat{p}_m \mid T)$ we have $\mathbb{E}(\hat{p}^\star_m) = p_m$ and

$$\mathbb{E}\{(\hat{p}^\star_m - p_m)^2\} \leq \mathbb{E}\{(\hat{p}_m - p_m)^2\}. \tag{31}$$

Moreover, we have

$$\hat{p}^\star_m = \frac{1}{n!} \sum_{\sigma \in S_n} \hat{p}_m\{X_{\sigma(1)}, \dots, X_{\sigma(n)}\}, \tag{32}$$

where S_n denotes the set of all permutations of $\{1, \dots, n\}$. An alternative expression for $\hat{p}^\star_m$ is

$$\hat{p}^\star_m = \frac{1}{\binom{n}{m}} \sum_{i=1}^{n} \binom{d_i}{m-1}, \tag{33}$$

where $d_i = \sum_{k=1}^n 1_{\{X_k < X_i\}}$ and $\binom{d_i}{m-1} = 0$ if $d_i < m-1$.

The above result shows that the estimator $\hat{p}^\star_m$ is superior to $\hat{p}_m$ in terms of mean squared error. From a numerical point of view, formula (33) is much more computationally efficient than (32). We shall refer to $\hat{p}^\star_m$ as to the sample concurrence probability bootstrap estimator. In Section 5, we provide simulations showing that the permutation bootstrap estimator $\hat{p}^\star_m$ has a significantly smaller variance than $\hat{p}_m$ and should hence be preferred. However, if the assumption of independent and identically distributed observations does not hold, the permutation bootstrap should be used with caution: simulations show that in presence of a trend, the permutation bootstrap can suffer from a significant bias—see Section 5.5.

4.4. A Connection to the Kendall's τ Estimator

As indicated in Corollary 3, in the case of max-stable data, the bias of the bivariate sample concurrence estimator can be corrected. Using the same trick again, in the case of pairwise concurrence we propose the following unbiased modification of $\hat{p}^\star_m$:

$$\tilde{p}^\star_m = \frac{m\hat{p}^\star_m - 1}{m-1}. \tag{34}$$

Surprisingly, when $m = 2$, the resulting estimator is nothing but the Kendall's τ.

Corollary 4. The estimator $\tilde{p}^\star_2 = 2\hat{p}^\star_2 - 1$ is equal to the sample Kendall's τ

$$\hat{\tau} = \frac{2}{n(n-1)} \sum_{1 \leq k < l \leq n} \times \text{sign}\{X_k(s_1) - X_l(s_1)\}\text{sign}\{X_k(s_2) - X_l(s_2)\}. \tag{35}$$

Observe that in the bivariate max-stable case, $\tilde{p}^\star_2$ is an unbiased estimator, so that $p = \mathbb{E}[\tilde{p}^\star_2] = \mathbb{E}[\hat{\tau}] = \tau$. We thus recover Theorem 3 with a different proof.

Proof of Corollary 4. When $m = 2$, Equation (33) reduces to

$$\hat{p}^\star_2 = \frac{2}{n(n-1)} \sum_{i=1}^{n} d_i,$$

and corresponds to the proportion of "concordant pairs." Since the Kendall's τ is equal to the difference of the proportions of concordant and discordant pairs, we have $\hat{\tau} = \hat{p}^\star_2 - (1 - \hat{p}^\star_2) = \tilde{p}^\star_2$. □

The sample Kendall's τ is known to be asymptotically normal (Dengler 2010, Theorem 4.3)

$$\sqrt{n}(\hat{\tau} - \tau) \longrightarrow N(0, \sigma_\tau^2),$$
$$\sigma_\tau^2 = 15\,\text{var}[F_{s_1,s_2}\{X(s_1), X(s_2)\} - F_{s_1}\{X(s_1)\} - F_{s_2}\{X(s_2)\}]. \tag{36}$$

Although the asymptotic variance σ_τ^2 is hard to evaluate as it requires knowledge of the dependence structure, in practice it can be accurately and consistently estimated using Jackknife (Schemper 1987), that is, by taking the empirical variance of the jackknife estimates

$$\begin{aligned}\hat{\tau}_{-\ell} &= \frac{1}{(n-1)(n-2)} \sum_{\substack{1 \leq i,j \leq n \\ i,j \neq \ell}} \text{sign}\{X_i(s_1) - X_j(s_1)\} \\ &\quad \times \text{sign}\{X_i(s_2) - X_j(s_2)\} \\ &= \frac{1}{(n-1)(n-2)} \Bigg[n(n-1)\hat{\tau} - 2\sum_{i=1}^{n} \text{sign}\{X_i(s_1) \\ &\quad - X_\ell(s_1)\}\text{sign}\{X_i(s_2) - X_\ell(s_2)\} \Bigg],\end{aligned}$$

where $\ell = 1, \dots, n$. That is,

$$\hat{\sigma}_\tau^2 = \frac{1}{n} \sum_{\ell=1}^{n} (\hat{\tau}_{-\ell} - \hat{\tau})^2 \to \sigma_\tau^2,$$

in probability. This implies that the classic large sample confidence intervals based on (36) with σ_τ replaces by $\hat{\sigma}_\tau$ are consistent.

4.5. Hypothesis Testing

Motivated by the application in Section 6, we want to assess whether the concurrence probability varies over time. Let $p(s_1, s_2, t)$ be the concurrence probability for locations $s_1, s_2 \in \mathcal{X}$ and time $t \in T$. Given two disjoint time periods $T_1, T_2 \subseteq T$, assume that $p(s_1, s_2, t) = p_1(s_1, s_2)$ for all $t \in T_1$ and similarly for the time period T_2. Then one might be interested in testing

$$H_0 : p_1(s_1, s_2) = p_2(s_1, s_2) \qquad H_1 : p_1(s_1, s_2) \neq p_2(s_1, s_2).$$

Using (36), it is straightforward to derive such a statistical test since, under the null hypothesis, we have

$$T = \frac{\hat{p}_1(s_1, s_2) - \hat{p}_2(s_1, s_2)}{\sqrt{\widehat{\sigma_1^2} + \widehat{\sigma_2^2}}} \xrightarrow{\text{d}} N(0, 1), \qquad n \to \infty,$$

where $\hat{p}_1(s_1, s_2)$, $\hat{p}_2(s_1, s_2)$, $\widehat{\sigma_1^2}$, and $\widehat{\sigma_2^2}$ are, respectively, the concurrence probability estimators for the time periods T_1 and T_2 and their corresponding estimated variances—obtained using the Jackknife procedure introduced above.

Remark 6. Note however that deriving a statistical test to assess whether the area of concurrence cell varies in time is much more complicated since it requires the characterization of the distribution of $\int_{s \in \mathcal{X}} \hat{p}(s_0, s) ds$, which is beyond the scope of the present work.

5. Simulation Study

In this section, we analyze the performance of the sample concurrence probability estimators $\hat{p}_m$, $\hat{p}_m^\star$, and $\tilde{p}_m^\star$ defined in (28), (33), and (34), respectively, and that of the Kendall's τ estimator $\hat{\tau}$ defined in (35). We discuss the role of the max-stability assumption and focus mainly on the bivariate case. Higher order concurrence probabilities are discussed in Section 5.4.

5.1. The Effect of the Permutation Bootstrap

We first focus on the sample concurrence probability estimators, $\hat{p}_m$ and its permutation bootstrap version $\hat{p}_m^\star$. Their performance are assessed with respect to the block size m and the sample size n. We use here observations from a max–stable Brown– Resnick model and use the exact simulation methodology of Dombry, Engelke, and Oesting (2016). Figure 2 shows the evolution of the root mean squared error as the block size grows. As expected, both estimators become increasingly more efficient as the sample size grows and, as expected from (31), the permutation estimator $\hat{p}_m^\star$ is more efficient than $\hat{p}_m$, independently of the block size m and the sample size n. The circles on the plot indicate the asymptotically optimal block size in (30), which are valid only for max-stable data. As expected the observed optimal block sizes are in good agreement with the theoretical ones. In practice, however, since the data are not exactly max-stable, we recommend using slightly larger values of m so as to ensure that the block-maxima are closer to a max-stable model but also to take into account that data usually exhibit serial dependence, for example, daily observations.

5.2. Robustness of Kendall's τ With Respect to Max-Stability

The consistency and asymptotic normality of Kendall's τ estimator $\hat{\tau}$ for bivariate concurrence probability assume that the observations are taken from a max-stable model. To assess the effect of max-stability, we perform a simulation study with observations that are not max-stable but only in the

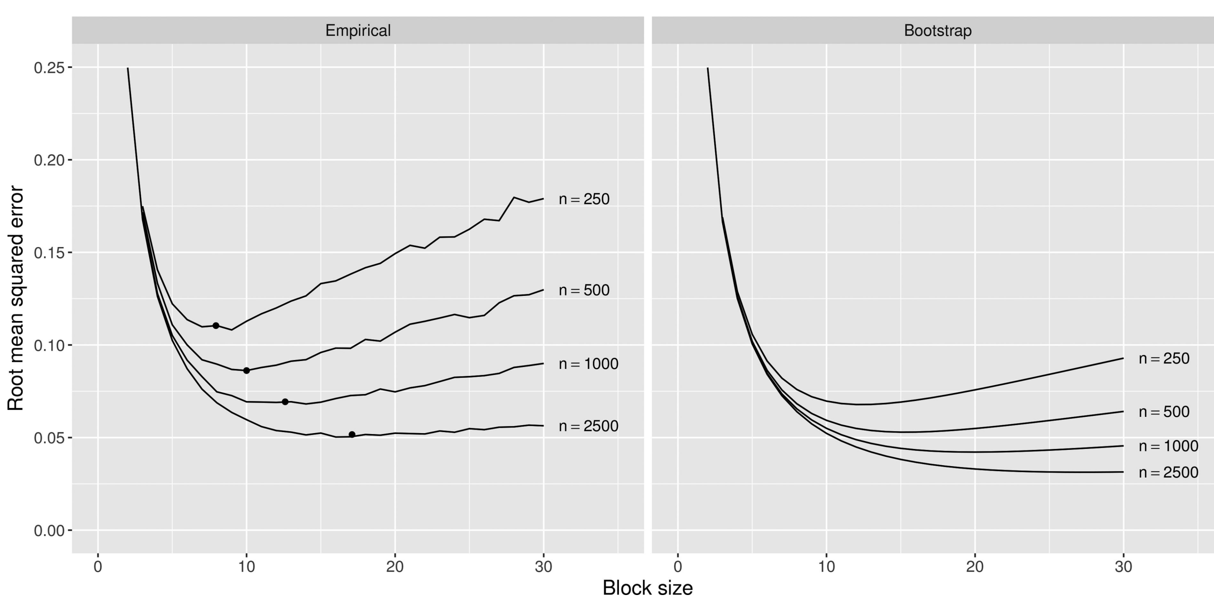

Figure 2. Evolution of the root mean squared error for $\hat{p}_m$ (left) and $\hat{p}_m^\star$ (right) as the block size m and the sample size n increase. These estimates were obtained from 2000 Monte Carlo samples sampled from a Brown–Resnick model with semivariogram $\gamma(h) = h/1.627$. This semivariogram was chosen such that the theoretical extremal concurrence probability is $p(h) = 0.5$ when $h = 1$. The points indicate the optimal block sizes as defined by (30) and their corresponding optimal root mean squared error (29).

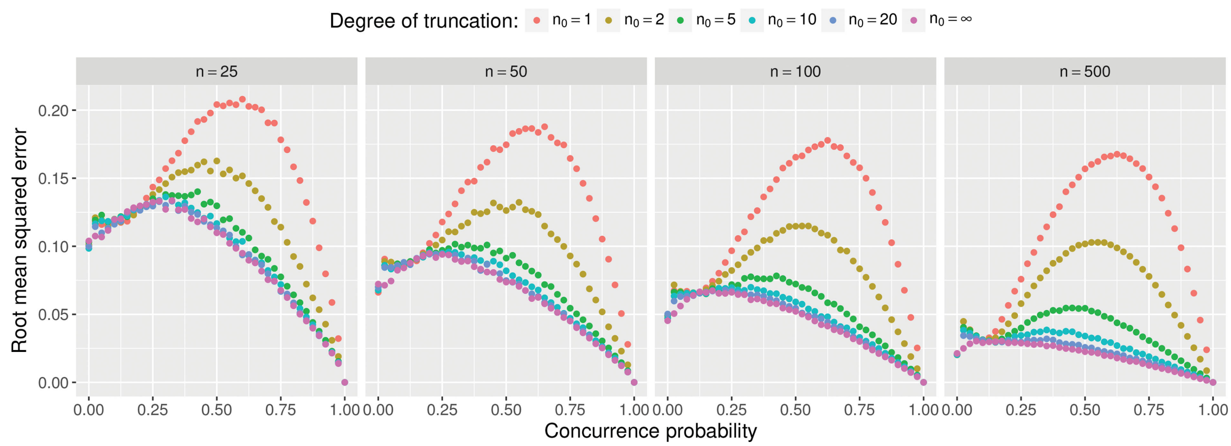

Figure 3. Evolution of the root mean squared error for $\hat{\tau}$ as the theoretical extremal concurrence probability p and the number of spectral function n_0 in (37) increase. These estimates were obtained from 2000 Monte Carlo samples of size n with, from left to right, $n = 25, 50, 100, 500$.

max-domain of attraction. Sampling from processes in the max-domain of attraction can be done in various ways, we propose here the following methodology that allows to control the extent to which the model differs from a max-stable one. Consider the partial maxima

$$\tilde{\eta}_{n_0}(s) = \frac{1}{n_0} \max_{i=1,\ldots,n_0} U_i^{-1} Y_i(s), \qquad s \in \mathcal{X}, \qquad (37)$$

where Y_i are as in (5), $U_1, \ldots, U_{n_0}$ independent $U(0,1)$ random variables and for some suitable $n_0 \in \mathbb{N}$. By construction, $\tilde{\eta}_{n_0}$ belongs to the max-domain of attraction of η in (5) and in some sense can be viewed as a *truncation* of the spectral representation in (5) (see, e.g., the proof of Proposition 3.1 in Stoev and Taqqu 2005). The larger the value of n_0, the closer the distributions of $\tilde{\eta}_{n_0}$ and η.

Figure 3 shows the evolution of the root mean squared error as the number of spectral functions n_0 in (37) and the theoretical extremal concurrence probability increase. As expected, as the sample size n grows, the estimator $\hat{\tau}$ becomes much more efficient. Interestingly, for small sample sizes, $\hat{\tau}$ appears to be fairly robust to the lack of max-stability in the data, that is, $n_0 < \infty$. This is not true anymore for larger sample sizes since, as expected, $\hat{\tau}$ becomes increasingly more efficient as the number of spectral functions increases.

5.3. Comparison of the Different Estimators

We compare the performance of the sample concurrence probability estimators $\hat{p}^\star_m$ and $\tilde{p}^\star_m$ in (33) and (34) and the Kendall's τ estimator $\hat{\tau}$ in (35). The sample concurrence estimators $\hat{p}^\star_m$ and $\tilde{p}^\star_m$ can be used for observations in the max-domain of attraction, provided the block size $m = m(n)$ scales suitably with respect to the number of observations. To compare the two types of estimators on a fair basis, we analyze their behavior when the simulated data are either perfectly max-stable or merely in the max-domain of attraction.

Figure 4 shows boxplots of the permutation bootstrap sample concurrence estimator $\hat{p}^\star_m$ and its unbiased version $\tilde{p}^\star_m$, as well as the Kendall's τ estimator $\hat{\tau}$, based on 2000 Monte Carlo realizations of both a Brown–Resnick and extremal-t models. Recall that we focus here on pairwise concurrence probabilities. As expected, the variability of all estimators decreases as the sample size grows; the Kendall's τ estimator being the most precise one. Since the simulated data are max-stable, we can see that the sample concurrence probability estimator is biased even when the sample size is large while the remaining two estimators are, as expected, unbiased. Overall the Kendall's τ appears to be the best estimator provided that the data are max-stable.

To corroborate this finding, Table 1 reports Monte Carlo sample means and standard deviations of these estimators as the assumption of max-stability becomes more reasonable, that is, as the number n_0 of spectral functions in (37) grows. As expected, when the max-stability assumption is most unreasonable, that is, $n_0 = 1$, all estimators show a substantial bias with the extremal concurrence probability estimator $\hat{\tau}$ having the largest bias while the unbiased sample one $\tilde{p}^\star_m$ the lowest. As the assumption of max-stability becomes increasingly more accurate, the bias of the unbiased sample concurrence and extremal concurrence estimators decrease. When this assumption holds exactly (indicated by $n_0 = \infty$), both of these estimators exhibit essentially no bias as stipulated by the theory and Figure 4. The sample concurrence probability estimator appears to be biased in all situations—the bias being less significant as the number of spectral functions is larger. Interestingly, whatever the estimator considered, the bias and variance appear to increase as the theoretical extremal concurrence probability value p becomes smaller. Overall the extremal concurrence probability estimator $\hat{\tau}$ in (35) has the lowest variability.

5.4. Simulation Study for Higher Order Concurrence Probabilities

For higher order concurrence probabilities, that is, $p(s_1, \ldots, s_k)$ with $k \geq 3$, estimation relies on the sample concurrence estimator $\hat{p}_m$ and its bootstrap version $\hat{p}^*_m$. The Kendall's τ estimator $\hat{\tau}$ and the unbiased version $\tilde{p}_m$ and $\tilde{p}^*_m$ of the sample concurrence estimators can be applied in the bivariate case $k = 2$ only (see Theorem 3 and Corollary 3).

Remark 7. Throughout the article, we put an emphasis on the bivariate case as this specific case is likely to be the most understandable in practice—for example, using the integrated concurrence probabilities of Proposition 3. However higher order

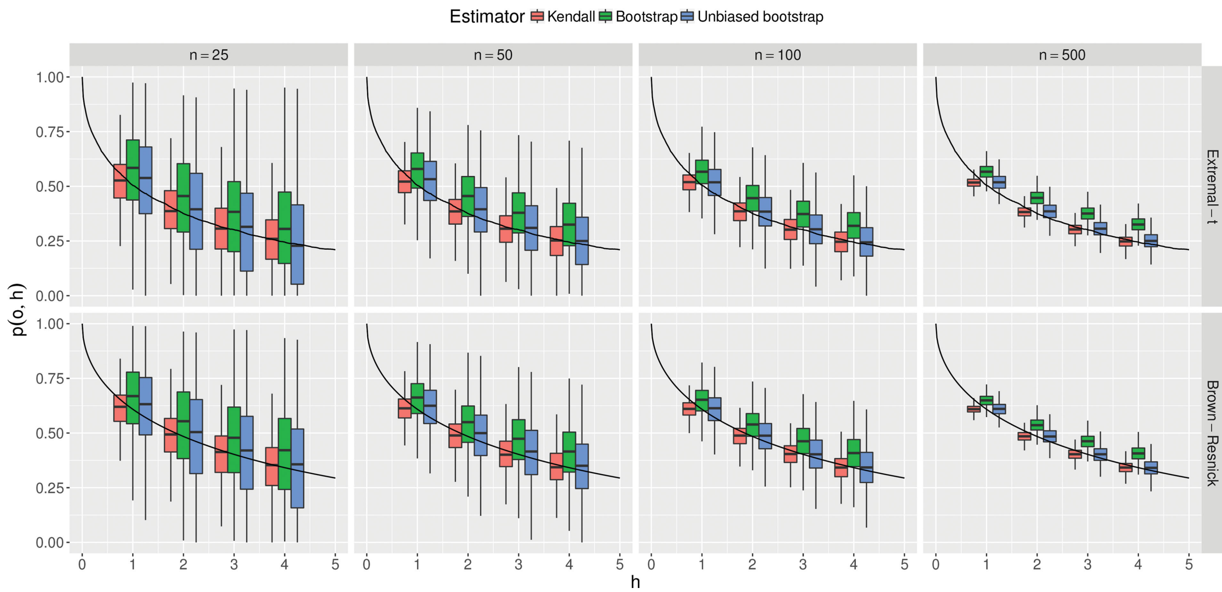

Figure 4. Boxplots of the Kendall's τ estimator $\hat{\tau}$ (red, left), and the bootstrap $\hat{p}^{\star}_m$ (green/middle) and unbiased bootstrap $\tilde{p}^{\star}_m$ (blue/right) concurrence probability estimators at distance lags $h = 1, 2, 3, 4$. The boxplots were obtained from 2000 independent estimates using max-stable data. From left to right: the sample size is, respectively, 25, 50, 100, and 500. The top panel corresponds to an extremal-t model with $\nu = 5$, and correlation function $\rho(h) = \exp(-h/10)$. The bottom panel corresponds to a Brown–Resnick model with semivariogram $\gamma(h) = h/3$. For each panel, the solid line represents the corresponding theoretical extremal concurrence probability function. Throughout this simulation study the block size is held fixed to $m = 10$, independently of the sample size n.

concurrence probabilities might still be of interest, for example, to compute the variance of the volume of the concurrence cell.

Estimation of high order concurrence probabilities is straightforward using estimator $\hat{p}^{\star}_m$. Table 2 summarizes the results of a simulation study based on a k-variate max-stable logistic model with dependence parameter $\alpha = 0.1, 0.5, 0.9$ and $k = 2, 10, 100$. From Example 1, we have $p(s_1, \dots, s_k) = \prod_{j=1}^{k-1}(1 - \alpha/j)$ so that $p_k \to 0$ as $k \to \infty$. We observe that $\hat{p}^{\star}_m$ is able to estimate $p(s_1, \dots, s_k)$ without any severe bias even in large dimension. However in the most critical situation, that is, $\alpha \approx 1$ and $k \gg 1$, the standard errors are typically of the same order as $p(s_1, \dots, s_k)$. Another simulation study (not presented here) with $\alpha = \alpha(k)$ depending on k in such a way that $p(s_1, \dots, s_k) = 0.5$ reveals that the estimation of k-variate extremal concurrence probabilities is just as efficient as in the bi-variate case.

Although the previous simulation study gives some insights about the behavior of the estimator in large dimension, the max-stable logistic model is not appropriate for modeling spatial extremes. We now investigate the case of infill asymptotics of a compact set $K \subset \mathcal{X}$. We focus on a sequence $K_\infty := \{s_k,\ k \in \mathbb{N}\}$ which is dense in K, that is, such that $K = \overline{K}_\infty$. Then, it follows that the sets $K_k := \{s_1, \dots, s_k\} \to K$, as $k \to \infty$ in the sense of the Fell, Painlevé–Kuratowski as well as in the Wijsman topologies, since all these topologies on closed sets coincide in Euclidean spaces (see, e.g., Theorem B.13 on p. 401 in

Table 1. Performance of the bootstrap ($\hat{p}^{\star}_m$), unbiased bootstrap ($\tilde{p}^{\star}_m$) concurrence probability estimators and the Kendall's τ ($\hat{\tau}$) estimator. The table reports the sample mean and the standard deviation in parentheses based on 2000 Monte Carlo replicates. The data are either simulated from an extremal-t model with correlation function $\rho(h) = \exp(-h/10)$ and $\nu = 5$ degrees of freedom or from its truncated representation with n_0 extremal functions. Throughout this simulation study the block size is held fixed to $m = 10$, independently of the sample size n.

	$p = 0.25$			$p = 0.50$			$p = 0.75$		
	$\hat{p}^{\star}_m$	$\tilde{p}^{\star}_m$	$\hat{\tau}$	$\hat{p}^{\star}_m$	$\tilde{p}^{\star}_m$	$\hat{\tau}$	$\hat{p}^{\star}_m$	$\tilde{p}^{\star}_m$	$\hat{\tau}$
				Sample size $n = 20$					
$n_0 = 1$	0.41 (0.24)	0.35 (0.26)	0.47 (0.13)	0.64 (0.22)	0.60 (0.24)	0.71 (0.09)	0.83 (0.15)	0.81 (0.17)	0.87 (0.05)
$n_0 = 10$	0.34 (0.24)	0.27 (0.25)	0.31 (0.14)	0.57 (0.23)	0.52 (0.26)	0.58 (0.12)	0.79 (0.17)	0.77 (0.19)	0.80 (0.07)
$n_0 = 15$	0.33 (0.24)	0.27 (0.25)	0.30 (0.15)	0.56 (0.23)	0.52 (0.26)	0.56 (0.12)	0.78 (0.17)	0.76 (0.19)	0.78 (0.07)
$n_0 = \infty$	0.33 (0.24)	0.27 (0.25)	0.25 (0.15)	0.55 (0.24)	0.50 (0.26)	0.50 (0.13)	0.77 (0.18)	0.75 (0.20)	0.75 (0.08)
				Sample size $n = 50$					
$n_0 = 1$	0.41 (0.13)	0.35 (0.14)	0.47 (0.08)	0.65 (0.10)	0.61 (0.12)	0.71 (0.05)	0.84 (0.07)	0.82 (0.07)	0.87 (0.03)
$n_0 = 10$	0.34 (0.13)	0.26 (0.14)	0.31 (0.09)	0.57 (0.12)	0.52 (0.13)	0.57 (0.07)	0.79 (0.08)	0.76 (0.09)	0.80 (0.04)
$n_0 = 15$	0.33 (0.13)	0.25 (0.14)	0.29 (0.09)	0.56 (0.12)	0.51 (0.13)	0.56 (0.07)	0.78 (0.08)	0.76 (0.09)	0.79 (0.04)
$n_0 = \infty$	0.32 (0.13)	0.25 (0.14)	0.24 (0.09)	0.54 (0.12)	0.49 (0.14)	0.50 (0.08)	0.77 (0.09)	0.74 (0.09)	0.75 (0.05)
				Sample size $n = 100$					
$n_0 = 1$	0.41 (0.08)	0.35 (0.09)	0.46 (0.06)	0.65 (0.07)	0.61 (0.07)	0.71 (0.03)	0.83 (0.04)	0.82 (0.04)	0.87 (0.02)
$n_0 = 10$	0.34 (0.09)	0.26 (0.10)	0.31 (0.06)	0.57 (0.08)	0.52 (0.09)	0.57 (0.05)	0.78 (0.05)	0.76 (0.05)	0.80 (0.03)
$n_0 = 15$	0.33 (0.09)	0.26 (0.10)	0.29 (0.06)	0.56 (0.08)	0.51 (0.09)	0.55 (0.05)	0.78 (0.05)	0.76 (0.06)	0.78 (0.03)
$n_0 = \infty$	0.33 (0.09)	0.25 (0.10)	0.25 (0.07)	0.55 (0.08)	0.50 (0.09)	0.50 (0.05)	0.78 (0.05)	0.75 (0.06)	0.75 (0.03)

Table 2. Performance of the permutation bootstrap estimator $\hat{p}^{\star}_m$. The table reports the sample mean and the standard deviation in parentheses based on 2000 Monte Carlo replicates. The data are simulated from a max-stable logistic distribution in dimension k with dependence parameter $\alpha \in \{0.1, 0.5, 0.9\}$. Throughout this simulation study the block size is held fixed to $m = 10$, independently of the sample size n.

	$\alpha = 0.1$			$\alpha = 0.5$			$\alpha = 0.9$		
n	$k = 2$ ($p = 0.90$)	$k = 10$ ($p \approx 0.75$)	$k = 100$ ($p \approx 0.60$)	$k = 2$ ($p = 0.50$)	$k = 10$ ($p \approx 0.19$)	$k = 100$ ($p \approx 0.06$)	$k = 2$ ($p = 0.10$)	$k = 10$ ($p \approx 0.014$)	$k = 100$ ($p \approx 0.0017$)
20	0.90 (0.11)	0.77 (0.16)	0.61 (0.20)	0.49 (0.27)	0.21 (0.22)	0.07 (0.14)	0.10 (0.23)	0.015 (0.069)	0.002 (0.023)
50	0.90 (0.05)	0.77 (0.07)	0.61 (0.10)	0.50 (0.14)	0.21 (0.12)	0.06 (0.08)	0.10 (0.12)	0.017 (0.043)	0.002 (0.016)
100	0.90 (0.03)	0.77 (0.04)	0.62 (0.06)	0.50 (0.09)	0.20 (0.08)	0.06 (0.05)	0.10 (0.08)	0.016 (0.028)	0.002 (0.010)
500	0.90 (0.01)	0.77 (0.02)	0.62 (0.03)	0.50 (0.04)	0.21 (0.03)	0.06 (0.02)	0.10 (0.04)	0.017 (0.013)	0.002 (0.004)
1000	0.90 (.007)	0.77 (0.01)	0.62 (0.02)	0.50 (0.03)	0.21 (0.02)	0.06 (0.02)	0.10 (0.03)	0.017 (0.009)	0.002 (0.003)

Molchanov 2005). If the limiting max-stable process has continuous paths (equivalently, its spectral functions are continuous—see Resnick and Roy 1991), by the monotone convergence theorem it follows that

$$p(s_1, \ldots, s_k) \longrightarrow p(K) = \mathbb{P}\{\text{for some } \ell \geq 1 : \eta(s) = \varphi_\ell(s), s \in K\}.$$

Thus, the limit $p(K)$ is naturally interpreted as the probability of extremal concurrence over K, see Remark 3.

We illustrate the above convergence by taking η to be a Brown–Resnick process on $\mathcal{X} = [0, T]$ with $\gamma(s) = s/3$ and $K_k = \{s_n = Tu_n : n = 1, \ldots, k\}$ where $\{u_n\}_{n\geq 1}$ is a Van der Corput sequence—that is, an equidistributed with low discrepancy sequence that is dense on $[0, 1]$. Figure 5 illustrates the performance of $\hat{p}^{*}_m(s_1, \ldots, s_k)$ as a function of k based on $n = 1000$ independent copies of η and block size $m = n^{1/3} = 10$. Pointwise sample mean and quantiles of order 0.025 and 0.975 are obtained from a Monte Carlo procedure using 2000 replicates while the limit theoretical value $p(\mathcal{X})$ is computed using (17). We observe that the concurrence probabilities quickly decreases for $k = 2, \ldots, 20$ and then reach a plateau. Since the block size is fixed to $m = 10$, we can observe a moderate bias. This limited experiment illustrates that concurrence probabilities over an interval or a region in $\mathbb{R}^d$ can be positive, and, depending on the model they could be rather large.

5.5. Model Misspecification: The Effect of a Linear Trend

Motivated by the application on continental US temperatures of Section 6, and to mimic a global warming effect, we investigate the impact of a linear trend on the proposed estimators. To this aim, we consider the time series model given by

$$X_t(s) = Z_t(s) + ct, \qquad t = 1, 2, \ldots, \qquad s \in \{0, 1\},$$

where the trend $c \in \mathbb{R}^2$ and $\{Z_t(0), Z_t(1), : t \geq 1\}$ is a sequence of independent copies of a max-stable logistic random variable whose marginal parameters were taken to be in agreement with that found in our US temperature application—that is, $\mu = 36$, $\sigma = 1.85$, and $\xi = -0.18$. Two different situations were considered: the trend coefficients $c = (\epsilon, \epsilon)^\top$ are both equal and positive; and when the trend coefficients $c = (\epsilon, -\epsilon)^\top$ have different signs, for some $\epsilon > 0$.

Figure 6 plots the bias of each estimator as the trend ϵ and the concurrence probability $p(0, 1)$ vary. Clearly only the sample concurrence estimator $\tilde{p}_m$ shows robustness against linear trends, while the two remaining estimators may be seriously impacted. Such a behavior was expected since $\hat{p}_m$ considers sample concurrence in successive blocks of (small) sizes m where it is likely that the linear trend will have a minor effect. It is not true anymore for both $\hat{p}^{\star}_m$ and $\hat{\tau}$ as they compare pairs of observations that can be far apart in time and for which the linear trend is likely to have a more pronounced impact.

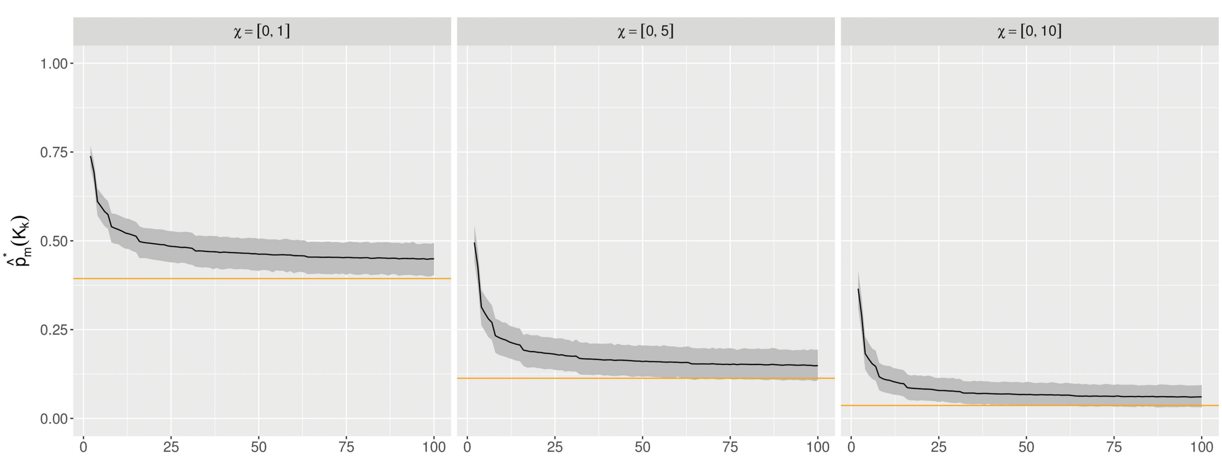

Figure 5. Behavior of the permutation bootstrap estimator $\hat{p}^{\star}_m(K_k)$ as $k \to \infty$ with $K_k = \{Tu_n : n = 1, \ldots, k\}$ and where $\{u_n : n \geq 1\}$ is the Van der Corput sequence on $[0, 1]$ and $T = 1, 5, 10$—left to right. Results are obtained from 2000 Monte Carlo replicates of 1000—sample from a Brown–Resnick process with semivariogram $\gamma(h) = h/3$. The (orange) horizontal lines correspond to the theoretical values $p(\mathcal{X})$ estimated using a Monte Carlo procedure.

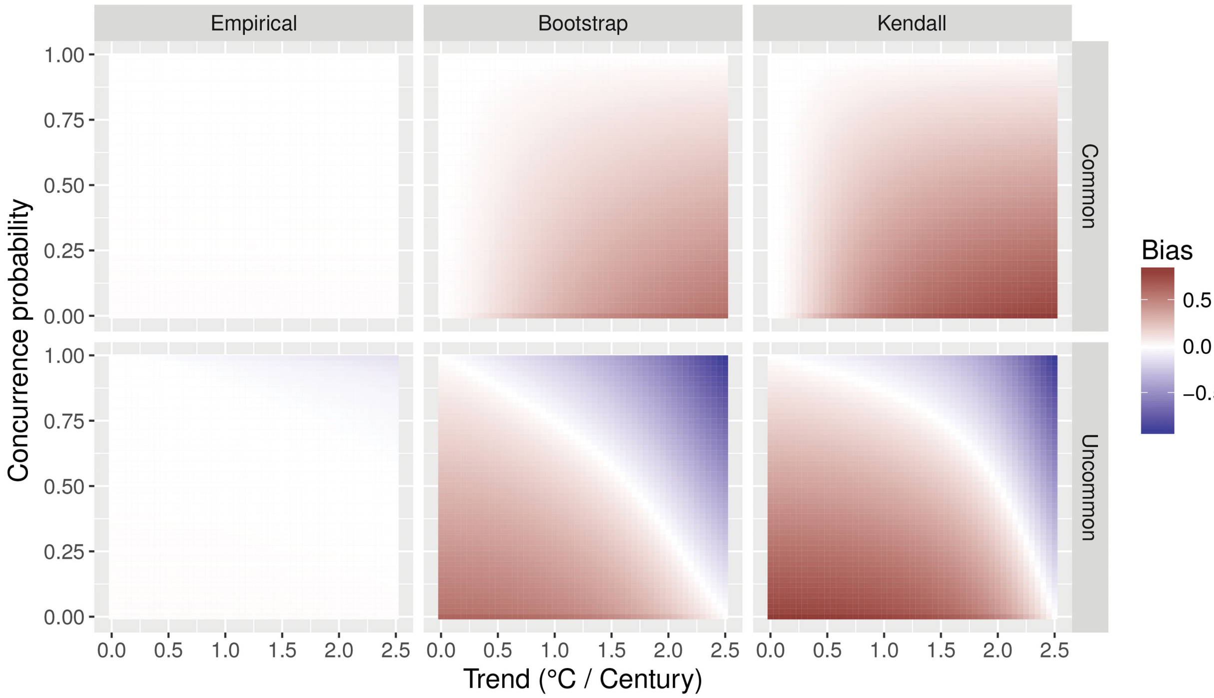

Figure 6. Impact of a linear trend on the empirical ($\hat{p}_m$), bootstrap ($\hat{p}^\star_m$), and Kendall's τ ($\hat{\tau}$) estimators. The top row shows results for a common trend while the bottom row investigates the case of opposite linear trends across the variables.

While $\hat{p}^\star_m$ and $\hat{\tau}$ have the smallest variance compared to that of $\hat{p}_m$, they are the least robust against linear trend misspecification. From a methodological point of view, this suggests a possible pretreatment of the data to remove any possible linear trend before using the better estimators $\hat{p}^\star_m$ and $\hat{\tau}$.

6. Concurrence of Temperature Extremes in Continental USA

In this section, we apply the developed methodology to estimate the probabilities of concurrence associated with extreme temperatures—both extreme cold and hot events. The data consist of daily temperature minima and maxima recorded at 424 weather stations over the period 1911–2010. The spatial distribution of these stations is given in Figure 7. This dataset, as a subset of the United States Historical Climatological Network (USHCN 2014), was chosen as it meets very high data quality standards and involves fewer than 2.4% missing values while spanning the entire territory of continental US. It can be freely downloaded from *http://cdiac.ornl.gov*.

To avoid any seasonal influence on our results, we decided to analyze minima and maxima for each season separately. We focus on the concurrence of extreme cold (minima) during the Fall and Winter seasons—generally color-coded in blue; and extreme hot (maxima) during the Spring and Summer seasons—generally color-coded in red. The right panel of Figure 7 shows the time series of these seasonal extrema for one particular weather station: Worland, Wyoming. We can see that all four time series of seasonal extremes appear to be stationary without any clear temporal trend. This is in contrast with the generally accepted trend of about 0.2°C per decade for average temperatures (Stocker et al. 2013).

Figure 8 plots the estimated spatial distribution of the extremal concurrence probabilities function for the Fall and Spring seasons for the time periods 1911–1950 and 1951–2010 and the associated p-values of the hypothesis test of any change in the pointwise concurrence probabilities between these two time periods—see Section 4.5. These concurrence probability maps were obtained by first computing the estimator (35) over all 423 pairs of stations (s_0, s), where s_0 denotes the spatial

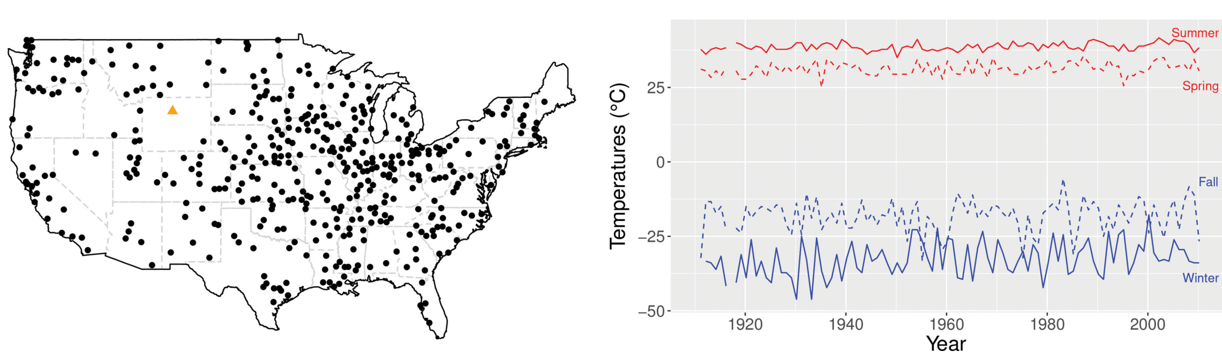

Figure 7. Left: Spatial distribution of the 424 weather stations. The triangle indicates the selected station for the analysis. Right: The seasonal extrema time series for the selected station.

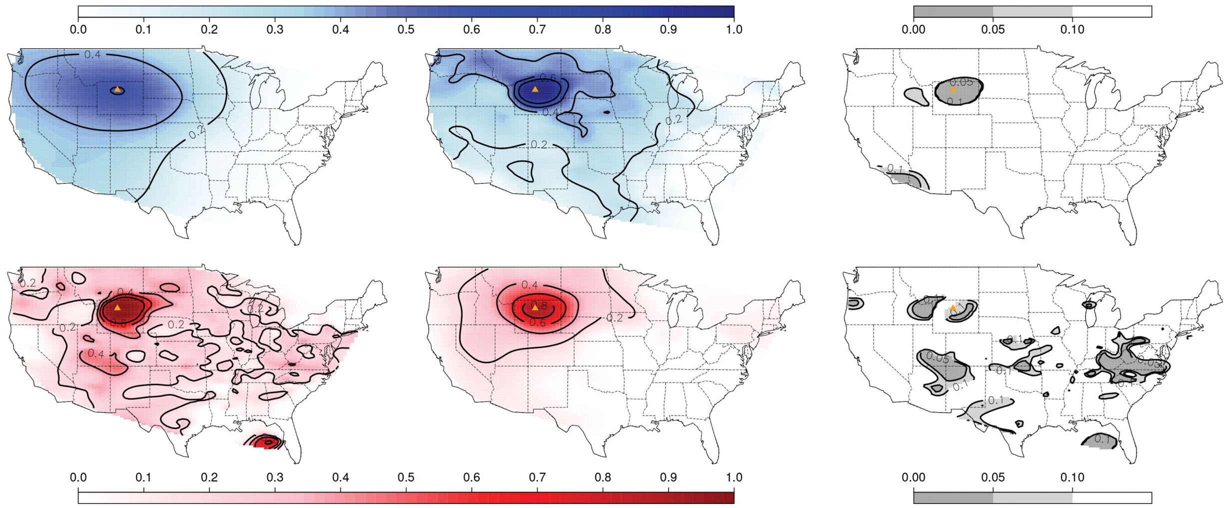

Figure 8. Maps of the extremal concurrence probability for the Worland station (triangle) for the Fall (top) and Spring (bottom) seasons. The left panels show results for the time period 1911–1950 while the middle panels to 1951–2010. The rightmost panels plot the pointwise p-values relative to the hypothesis test of concurrence probabilities difference between the two time periods—see Section 4.5.

coordinates of the Worland station, and then interpolated using thin plate splines (on logit scale) provided by the R package fields (Nychka et al. 2017). As expected, the highest concurrence probability occurs in the neighborhood of the selected station independently of the season. The areal extent of high concurrence probabilities, however, seems to be larger for minimum temperatures (cold extremes) than for maximum temperatures (hot extremes). This finding is consistent with the physical notion of entropy, that is, when the ambient temperature is higher (Spring and Summer seasons), the entropy is greater and hence involves less spatial dependence than for cooler temperatures leading to smaller probability of simultaneous extremes. This difference can be also attributed to the fact that extreme cold temperatures are often due to high-pressure systems, which tend to linger longer and cover a larger spatial area than warm fronts giving rise to concurrence of extreme hot events.

Although the concurrence probability maps for the time period 1911–1950 and 1951–2010 show very different patterns, the rightmost panels of Figure 8 suggest that these changes are only statistically significant on a small fraction of the US territory. However, these findings have to be nuanced by the fact that we are plotting pointwise p-values so that we are facing an infinite-dimensional multiple comparisons problem.

Although Figure 8 displays interesting patterns, it has the drawback of being dependent on the choice of the origin, that is, the selected station. However as stated in Section 2.5, it is possible to bypass this hurdle by focusing on concurrence cell instead. Figure 9 plots the differences in the spatial distribution of $\mathbb{E}\{|C(s|\}$ and $\mathrm{var}\{|C(s)|\}$ for the preindustrial period, that is, 1911–1950, and the postindustrial one, that is, 1951–2010. Overall we can see that during the last 60 years extremal concurrence cells appear to be larger and with an increased variability for cold seasons while it is the opposite for hot seasons. These findings indicate that today's climate shows cold spells that have a larger spatial impact than in the beginning of the 20th century while hot spells are more localized. Our results agree with the conclusions drawn by Field et al. (2012)

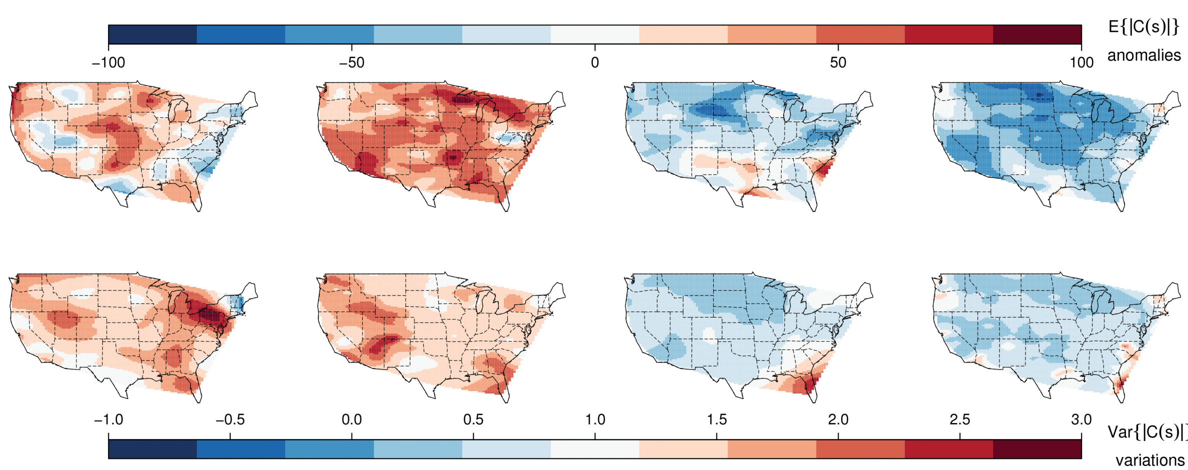

Figure 9. Top: Spatial distribution of the expected extremal concurrence cell areas anomalies, that is, the pointwise difference between $\mathbb{E}\{|C(s)|\}$ for period 1951–2010 and period 1911–1950. Bottom: Spatial distribution of the extremal concurrence cell area variations, that is, the pointwise ratio between $\mathrm{var}\{|C(s)|\}$ for period 1951–2010 and 1911–1950. Each column corresponds to one season. From left to right: Fall, Winter, Spring, and Summer.

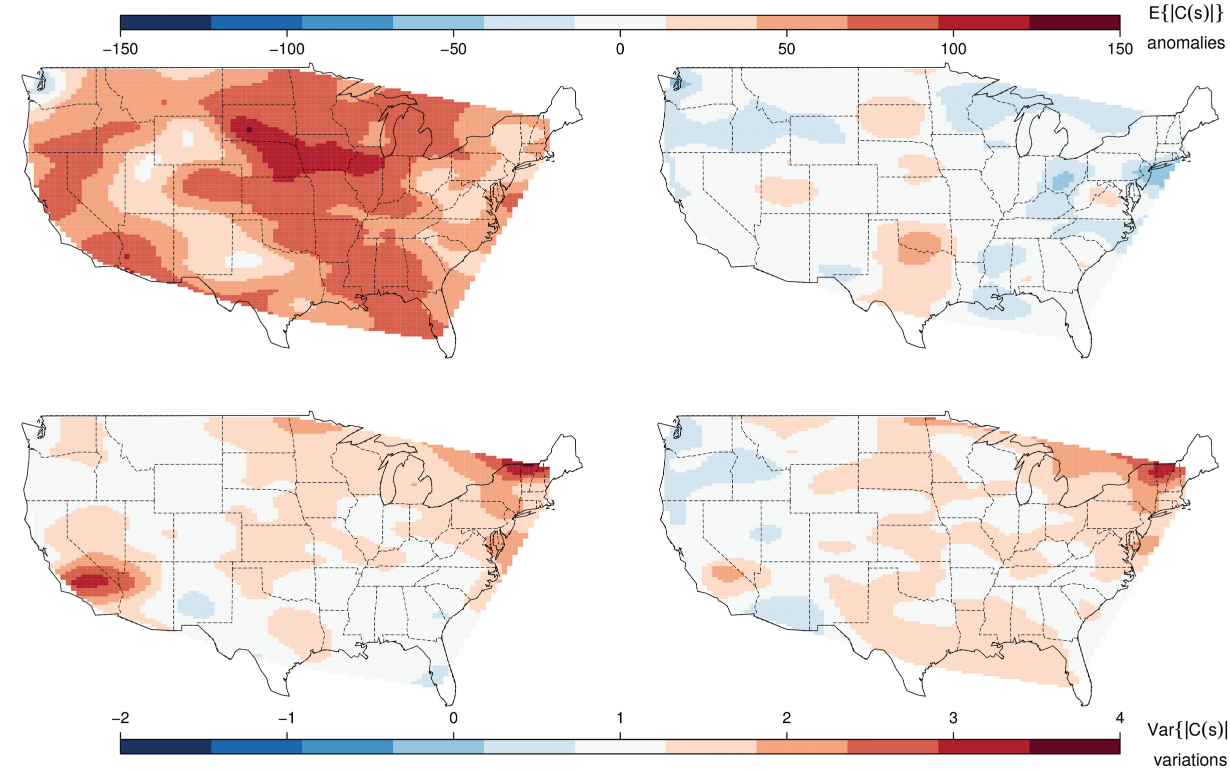

Figure 10. Top: Spatial distribution of the expected extremal concurrence cell area anomalies, that is, the pointwise difference between $\mathbb{E}\{|C(s)|\}$ for El Nio/La Nia years and La Nada years (left/right). Bottom: Spatial distribution of the extremal concurrence cell area variations, that is, the pointwise ratio between var$\{|C(s)|\}$ for El Nio/La Nia years and La Nada years (left/right). The focus here is on winter extremes (temperature minima).

who states that "there is evidence from observations gathered since 1950 of change in some extremes." These changes in the concurrence patterns of summer extremes can be attributed to global warming since an increase in entropy generally leads to more "mixing" in the system and hence less dependence leading to smaller areas of concurrence. The changes in concurrence patterns of extreme cold events, however, are harder to explain. They may be triggered by structural changes in important climatological mechanisms such as the Arctic Oscillation, for example.

Finally, we consider another cut of the data by stratifying according to an important climate phenomenon known as the El Nio Southern Oscillation (ENSO). Positive ENSO (El Nio) refers to the event of a warm-up of the surface water in the central and east-central equatorial Pacific ocean. It is well known that years with high ENSO have a general warming effect in North America during the winter season. The opposite effect of negative ENSO (La Nia) is characterized by a cool-down in the same area of the Pacific and it generally leads to unusually cold winters in the northwestern part of the US, northern California and the north-central states (Graham 1999). Figure 10 plots the changes in the mean and the variance of the concurrence cell area. The estimates reported here are the anomalies/variations compared to the base class "La Nada," that is, years that are not labeled as El Nio nor La Nia, for Winter minima. During the time period 1911–2010, there were, respectively, 29, 25, and 46 winter seasons classified as El Nio, La Nia, and La Nada. Overall, relative to La Nada, we can see that La Nia (right plots) does not seem to have an impact on the spatial coverage of winter minima though its variability seems to be a bit more pronounced in the East coast. On the other hand, El Nio (left plots) seems to induce more massive and volatile cold extremes over the whole USA.

7. Discussion

In this article, we introduce a new perspective to multivariate and spatial extremes based on the fundamental notion of concurrence. The extremal concurrence probability can be viewed as a measure of dependence, similar to the popular extremal coefficient function. It has the advantage, however, of being readily interpretable as the probability that a *single event* will cause the extremes over a region of interest. Theoretical properties and closed-form expressions of these concurrence probabilities have been established and several estimators have been proposed. In practice, the bi-variate concurrence probability is easily interpreted and provides means of computing expected areas of concurrence cells. Interestingly, for max-stable models, it reduces to the classic Kendall's τ. A simulation study has shown that the proposed estimators work well in practice and that they give a new insight into the dependence of extremes, as illustrated with an analysis of the areas of concurrence regions for temperature extremes in the continental USA.

Acknowledgments

The authors gratefully acknowledge the help of Prof. Paul H. Whitfield with the interpretation of the results on concurrence for temperature extremes and also for the suggestion to stratify by El Niño/La Niña effect.

Funding

M. Ribatet was partly funded by the MIRACCLE-GICC and McSim ANR projects. S. Stoev was partially funded by the NSF grant "FRG: Collaborative Research: Extreme value theory for spatially indexed functional data" DMS-1462368.

ORCID

Mathieu Ribatet http://orcid.org/0000-0003-0231-6001

References

Asadi, P., Davison, A., and Engelke, S. (2015), "Extremes on River Networks," *The Annals of Applied Statistics*, 9, 2023–2050. [1565]

Cooley, D., Naveau, P., and Poncet, P. (2006), "Variograms for Spatial Max-Stable Random Fields," in *Dependence in Probability and Statistics (Lecture Notes in Statistics*), Vol. 187), eds. P. Bertail, P. Soulier, P. Doukhan, P. Bickel, P. Diggle, S. Fienberg, U. Gather, I. Olkin, and S. Zeger, New York: Springer, pp. 373–390. [1567,1569]

Cooley, D., Nychka, D., and Naveau, P. (2007), "Bayesian Spatial Modeling of Extreme Precipitation Return Levels," *Journal of the American Statistical Association*, 102, 824–840. [1565]

Davison, A., Padoan, S., and Ribatet, M. (2012), "Statistical Modelling of Spatial Extremes," *Statistical Science*, 7, 161–186. [1565]

Davison, A. C., and Gholamrezaee, M. M. (2011), "Geostatistics of Extremes," *Proceedings of the Royal Society A: Mathematical, Physical and Engineering Science*, vol. 468, pp. 581–608. [1565]

de Haan, L. (1984), "A Spectral Representation for Max-Stable Processes," *The Annals of Probability*, 12, 1194–1204. [1567,1568]

de Haan, L., and Ferreira, A. (2006), *Extreme Value Theory (Springer Series in Operations Research and Financial Engineering)*, New York: Springer. [1565]

Dengler, B. (2010), "On the Asymptotic Behavior of Kendall's Tau," Ph.D. dissertation, Vienna University of Technology, Vienna, Austria. Available at *http://www.ub.tuwien.ac.at/diss/AC07806793.pdf*. [1573]

Dombry, C., Engelke, S., and Oesting, M. (2016), "Exact Simulation of Max-Stable Processes," *Biometrika*, 103, 303–317. [1574]

Dombry, C., and Éyi-Minko, F. (2013), "Regular Conditional Distributions of Max Infinitely Divisible Random Fields," *Electronic Journal of Probability*, 18, 1–21. [1567]

Dombry, C., Éyi-Minko, F., and Ribatet, M. (2013), "Conditional Simulations of Max-Stable Processes," *Biometrika*, 100, 111–124. [1565,1567]

Dombry, C., Falk, M., and Zott, M. (2015), "On Functional Records and Champions," *Journal of Theoretical Probability*, preprint. [1568]

Dombry, C., and Kabluchko, Z. (2017), "Random Tessellations Associated With Max-Stable Random Fields," *Bernoulli*, 24, 30–52. [1570]

Engelke, S., Malinowski, A., Kabluchko, Z., and Schlather, M. (2015), "Estimation of Hüsler-Reiss Distributions and Brown-Resnick Processes," *Journal of the Royal Statistical Society*, Series B, 77, 239–265. [1566]

Field, C., Barros, V., Stocker, T., Qin, D., Dokken, D., Ebi, K., Mastrandrea, M., Mach, K., Plattner, G.-K., Allen, S., Tignor, M., and Midgley, P. (eds.) (2012), *IPCC, 2012: Managing the Risks of Extreme Events and Disasters to Advance Climate Change Adaptation. A Special Report of Working Groups I and II of the Intergovernmental Panel on Climate Change*, Cambridge, UK; New York, NY, USA: Cambridge University Press. [1579]

Finkenstädt, B., and Rootzén, H. (eds.) (2004), *Extreme Values in Finance, Telecommunications, and the Environment* (*Monographs on Statistics and Applied Probability*, Vol. 99), New York: Chapman and Hall/CRC. [1565]

Ghoudi, K., Khoudraji, A., and Rivest, L.-P. (1998), "Propriétés Statistiques Des Copules de Valeurs Extrêmes Bidimensionnelles," *Canadian Journal of Statistics*, 26, 187–197. [1569]

Gnedin, A. V. (1993), "On Multivariate Extremal Processes," *Journal of Multivariate Analysis*, 46, 207–213. [1566]

——— (1994), "On a Best-Choice Problem With Dependent Criteria," *Journal of Applied Probability*, 31, 221–234. [1566]

——— (1998), "Records From a Multivariate Normal Sample," *Statistics & Probability Letters*, 39, 11–15. [1566]

Graham, S. (1999), "NASA: Earth Observatory," available at *http://earthobservatory.nasa.gov/Features/LaNina/* [1580]

Hashorva, E., and Hüsler, J. (2005), "Multiple Maxima in Multivariate Samples," *Statistics & Probability Letters*, 75, 11–17. [1566,1568]

Kabluchko, Z. (2009), "Spectral Representations of Sum- and Max-Stable Processes," *Extremes*, 12, 401–424. [1568]

Kabluchko, Z., Schlather, M., and de Haan, L. (2009), "Stationary Max–Stable Fields Associated to Negative Definite Functions," *Annals of Probability*, 37, 2042–2065. [1565,1571]

Leadbetter, M. R., Lindgren, G., and Rootzén, H. (1983), *Extremes and Related Properties of Random Sequences and Processes*, New York: Springer-Verlag. [1565]

Ledford, A. W., and Tawn, J. A. (1998), "Concomitant Tail Behaviour for Extremes," *Advances in Applied Probability*, 30, 197–215. [1566]

Molchanov, I. (2005), *Theory of Random Sets* (*Probability and its Applications)*, London: Springer-Verlag London Ltd. [1577]

Nychka, D., Furrer, R., Paige, J., and Sain, S. (2017), *Fields: Tools for Spatial Data, R Package Version 9.6*, Boulder, CO: University Corporation for Atmospheric Research. [1579]

Oesting, M., Bel, L., and Lantuéjoul, C. (2018), "Sampling From a Max-Stable Process Conditional on a Homogeneous Functional with an Application for Downscaling Climate Data," *Scandinavian Journal of Statistics*, 45, 382–404. [1565]

Oesting, M., and Schlather, M. (2013), "Conditional Sampling for Max-Stable Processes With a Mixed Moving Maxima Representation," *Extremes*, 17, 157–192. [1565]

Opitz, T. (2013), "Extremal t Processes: Elliptical Domain of Attraction and a Spectral Representation," *Journal of Multivariate Analysis*, 122, 409–413. [1565]

Padoan, S., Ribatet, M., and Sisson, S. (2010), "Likelihood-Based Inference for Max-Stable Processes," *Journal of the American Statistical Association (Theory & Methods)*, 105, 263–277. [1565,1571]

Penrose, M. D. (1992), "Semi-Min-Stable Processes," *Annals of Probability*, 20, 1450–1463. [1567]

Reich, B. J., and Shaby, B. A. (2012), "A Hierarchical Max-Stable Spatial Model for Extreme Precipitation," *Annals of Applied Statistics*, 6, 1430–1451. [1565]

Resnick, S., and Roy, R. (1991), "Random USC Functions, Max-Stable Processes and Continuous Choice," *The Annals of Applied Probability*, 1, 267–292. [1567,1577]

Resnick, S. I. (1987), *Extreme Values, Regular Variation and Point Processes*, New York: Springer-Verlag. [1565,1567,1570]

Ribatet, M. (2013), "Spatial Extremes: Max-Stable Processes at Work," *Journal de la Société Française de Statistique*, 154, 156–177. [1565]

Samorodnitsky, G., and Taqqu, M. S. (1994), *Stable Non-Gaussian Processes: Stochastic Models with Infinite Variance*, New York, London: Chapman and Hall. [1570]

Schemper, M. (1987), "Nonparametric Estimation of Variance, Skewness and Kurtosis of the Distribution of a Statistic by Jackknife and Bootstrap Techniques," *Statistica Neerlandica*, 41, 59–64. [1573]

Schlather, M. (2002), "Models for Stationary Max-Stable Random Fields," *Extremes*, 5, 33–44. [1565,1567]

Schlather, M., and Tawn, J. (2003), "A Dependence Measure for Multivariate and Spatial Extremes: Properties and Inference," *Biometrika*, 90, 139–156. [1567,1569]

Schneider, R., and Weil, W. (2008), *Stochastic and Integral Geometry (Probability and its Applications)*, Berlin: Springer-Verlag. [1568]

Smith, R. L. (1990), "Max-Stable Processes and Spatial Extreme," unpublished manuscript. Available at: *http://www.stat.unc.edu/postscript/rs/spatex.pdf*. [1567]

Stephenson, A., and Tawn, J. (2005), "Exploiting Occurrence Times in Likelihood Inference for Componentwise Maxima," *Biometrika*, 92, 213–227. [1566]

Stocker, T., Qin, D., Plattner, G.-K., Tignor, M., Allen, S., Boschung, J., Nauels, A., Xia, Y., Bex, V., and Midgley, P. (eds.) (2013), *IPCC, 2013: Climate Change 2013: The Physical Science Basis. Contribution of Working Group I to the Fifth Assessment Report of the Intergovernmental Panel on Climate Change*, Cambridge, United Kingdom and New York, NY, USA: Cambridge University Press. [1578]

Stoev, S. A. (2008), "On the Ergodicity and Mixing of Max-Stable Processes," *Stochastic Processes and their Applications*, 118, 1679–1705. [1567]

Stoev, S., and Taqqu, M. S. (2005), "Extremal Stochastic Integrals: A Parallel Between Max–Stable Processes and $\alpha-$stable Processes," *Extremes*, 8, 237–266. [1568,1575]

USHCN (2014), "United States Historical Climatological Network: Daily Temperature Extremes for the Period 1911–2010 in Continental USA," Available at *http://cdiac.ornl.gov/ftp/us_recordtemps/sta424/* [1578]

Wadsworth, J. L. (2015), "On the Occurrence Times of Componentwise Maxima and Bias in Likelihood Inference for Multivariate Max-Stable Distributions," *Biometrika*, 102, 705–711. [1566]

Wadsworth, J. L., and Tawn, J. A. (2014), "Efficient Inference for Spatial Extreme Value Processes Associated to Log-Gaussian Random Functions," *Biometrika*, 101, 1–15. [1565,1566]

Wang, Y., and Stoev, S. A. (2011a), "Conditional Sampling for Spectrally Discrete Max-Stable Random Fields," *Advances in Applied Probability*, 43, 461–483. [1565]

———, and Stoev, S. A. (2011b), "Conditional Sampling for Spectrally Discrete Max-Stable Random Fields," *Advances in Applied Probability*, 443, 461–483. [1567]

Weintraub, K. S. (1991), "Sample and Ergodic Properties of Some Min–Stable Processes," *The Annals of Probability*, 19, 706–723. [1567]